Table II. *Suppression of EAE induction in CBF$_1$ mice treated with ES-DC*[a]

Treatment (ES-DC)	Disease Incidence	Day of Onset	Mean Peak Clinical Score
No Treatment (control)	26/26	10.5 ± 1.1	3.3 ± 0.4
Pre[b]- TRAIL/MOG	**3/10**	18.3 ± 2.4	**0.3 ± 0.4**
Pre- PD-L1/MOG	**5/10**	13.4 ± 2.1	**0.8 ± 0.8**
Pre- MOG	8/8	10.5 ± 1.3	3.0 ± 0.3
Pre- TRAIL/OVA	6/6	10.2 ± 2.9	3.0 ± 0
Pre- PD-L1/OVA	6/6	11.3 ± 0.9	3.0 ± 0
Pre- TRAIL + MOG	6/6	10.2 ± 1.2	3.2 ± 0.6
Pre- PD-L1 + MOG	6/6	10.2 ± 0.6	3.3 ± 0.7
Post[c]- TRAIL/MOG	**3/6**	18.7 ± 4.4	**0.5 ± 0.5**
Post- PD-L1/MOG	**3/6**	13.7 ± 1.1	**1.0 ± 1.0**
Post- MOG	6/6	10.8 ± 1.0	3.2 ± 0.3

[a] Data are combined from a total of 10 separate experiments including those shown in Figs. 6 and 7. EAE was induced by s.c. injection at the tail base of a 0.2-ml IFA/PBS solution containing 400 μg of *M. tuberculosis* and 600 μg of MOG peptide once (on day 0), together with i.p. injections of 500 ng of purified *B. pertussis* toxin on days 0 and 2. For prevention of EAE, mice were injected i.p. with ES-DC (1 × 10^6 cells/mouse/injection) [b]on days −8, −5, and −2 (preimmunization treatment), or [c]on days 5, 9, and 13 (postimmunization treatment).

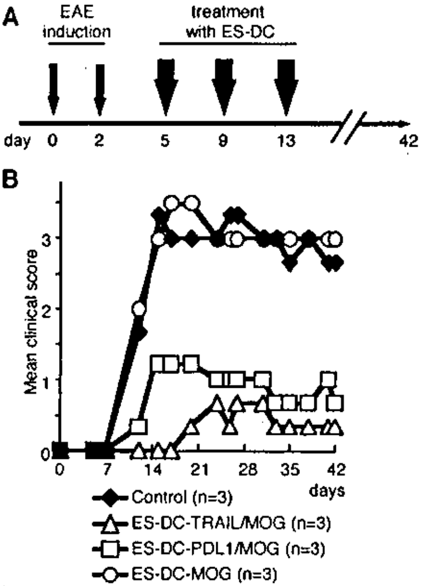

FIGURE 7. Inhibition of MOG-induced EAE by treatment with ES-DC expressing MOG plus TRAIL or MOG plus PD-L1 after immunization with MOG. *A*, The schedule for induction of EAE and treatment is shown. CBF$_1$ mice (three mice per group) were immunized on days 0 and 2 according to the EAE induction schedule described above, and subsequently i.p. injected with ES-DC (1 × 10^6 cells/injection/mouse) on days 5, 9, and 13. *B*, Disease severity of mice treated with ES-DC-TRAIL/MOG, ES-DC-PD-L1/MOG, ES-DC-MOG, or RPMI 1640 medium (control) is shown. The data are each representative of two independent and reproducible experiments, and data of all experiments are summarized in Table II.

such genetically modified ES-DC did not affect the immune response to irrelevant Ags.

We immunohistochemically analyzed spinal cord, the target organ of the disease, of mice subjected to EAE induction with or without treatment with ES-DC. Massive infiltration of CD4$^+$ T cells, CD8$^+$ T cells, and Mac-1$^+$ macrophages was observed in spinal cords of untreated control mice (Fig. 9). In contrast, T cells and macrophages hardly infiltrated into the spinal cord of mice treated with ES-DC-TRAIL/MOG or ES-DC-PD-L1/MOG. The results of histological analysis are in parallel with the severity of EAE and activation state of MOG-specific T cells of each mouse.

Increased number of apoptotic cells in splenic CD4$^+$ T cells by treatment with ES-DC-TRAIL/MOG

With regard to the mechanism of prevention of EAE by transfectant ES-DC, we analyzed the apoptosis of CD4$^+$ T cell in spleens of mice treated with ES-DC by staining with annexin V and subsequent flow-cytometric analysis. In the results, we observed that transfer of ES-DC-TRAIL/MOG caused an increase of apoptosis of CD4$^+$ T cells in recipient mice (17.3 ± 2.5%), compared with transfer of ES-DC-MOG (12.0 ± 0.4%), ES-DC-PD-L1/MOG (12.2 ± 0.5%), or RPMI 1640 medium control (10.2 ± 0.8%). In the experiments, three mice were used for each group. Increased numbers of apoptotic cells in spleen of mice transferred with ES-DC-TRAIL/MOG were also observed in histological analysis with TUNEL staining (Fig. 10). The capacity of ES-DC-TRAIL/MOG to cause apoptosis of T cells may play some role in the protection from EAE.

Discussion

DC are the most potent APC responsible for priming of naive T cells in initiation of the immune response. Recent studies revealed that DC are also involved in the maintenance of immunological self-tolerance, promoting T cells with regulatory functions, or inducing anergy of T cells. In vivo transfer of Ag-loaded DC with a tolerogenic character is regarded as a promising therapeutic means to negatively manipulate immune response in an Ag-specific manner. Various culture procedures used to generate DC with a tolerogenic character have been reported (31–36). Mouse bone marrow-derived DC generated in the presence of IL-10 and/or TGF-β or in the low dose of GM-CSF showed immature phenotypes, a low-level expression of cell surface MHC and costimulatory molecules, and induced T cell anergy in vitro and tolerance to specific Ags or allogeneic transplanted organs in vivo. In human monocyte-derived immature DC loaded with antigenic peptides and transferred in vivo have been shown to cause the Ag-specific immune suppression (37).

AQ:

Genetic modification may be a more steady and reliable way to manipulate the character of DC. Generation of tolerogenic DC by forced expression of Fas ligand, indoleamine 2,3-dioxygemase, IL-10, or CTLA4Ig by gene transfer has been also reported (38–41). In a recent study, type II collagen-loaded bone marrow-derived DC genetically engineered to express TRAIL by using an adenovirus vector ameliorated type II collagen-induced arthritis (42).

Regarding methods for gene transfer to DC, electroporation, lipofection, and virus vector-mediated transfection have been reported (38–43). However, considering clinical applications, presently established methods have several drawbacks, i.e., efficiency of gene transfer, stability of gene expression, limitation of the size and number of genes to be introduced, potential risk accompanying the use of virus vectors, and the immunogenicity of the virus vectors. For the purpose of Ag-specific negative regulation of immune responses, the antigenicity of vector systems may lead to problems. Importantly, to efficiently down-modulate T cell responses in an Ag-specific manner, it is desirable to introduce multiple expression vectors to generate stable transfectant DC, which continuously present transgene-derived Ag and simultaneously express immunosuppressive molecules.

Efficient genetic modification of mouse DC can be done by gene transfer to ES cells and subsequent differentiation of transfectant ES cells to ES-DC. By sequential transfection of ES cells using multiple expression vectors, transfectant ES-DC expressing multiple transgene products can readily be generated. In a recent study,

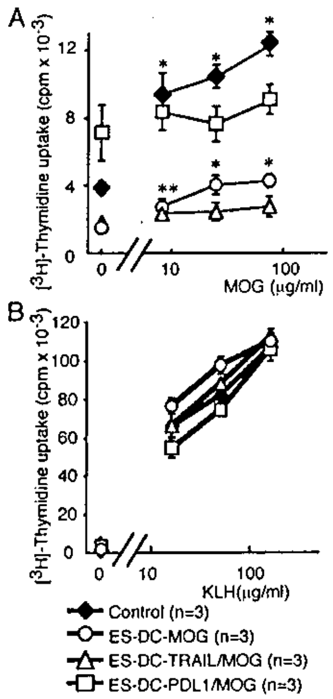

FIGURE 8. Inhibition of activation of MOG-reactive T cells and no effect of activation of KLH-specific T cell by treatment of mice with ES-DC expressing MOG plus TRAIL or PD-L1. *A*, Inguinal lymph node cells (3×10^5) were isolated from CBF$_1$ mice (three mice per group) of various treatment groups at over day 42, and were stimulated ex vivo with irradiated and MOG peptide-pulsed syngeneic spleen cells for 3 days. Proliferative response of T cells was quantified by [^{3}H]thymidine uptake in the last 12 h of the culture. The asterisks indicate that the differences in responses are statistically significant compared with count in the absence of Ag (*, $p < 0.01$; **, $p < 0.05$). The data are each representative of two independent and reproducible experiments with similar results. *B*, CBF$_1$ mice (three mice per group) were i.p. injected with ES-DC (1×10^6 cells/injection/mouse) on days −8, −5, and −2, and immunized with KLH/CFA on day 0. On day 11, inguinal lymph node cells were isolated and restimulated with the indicated concentration of KLH in vitro. Proliferation of T cells was quantified as described above.

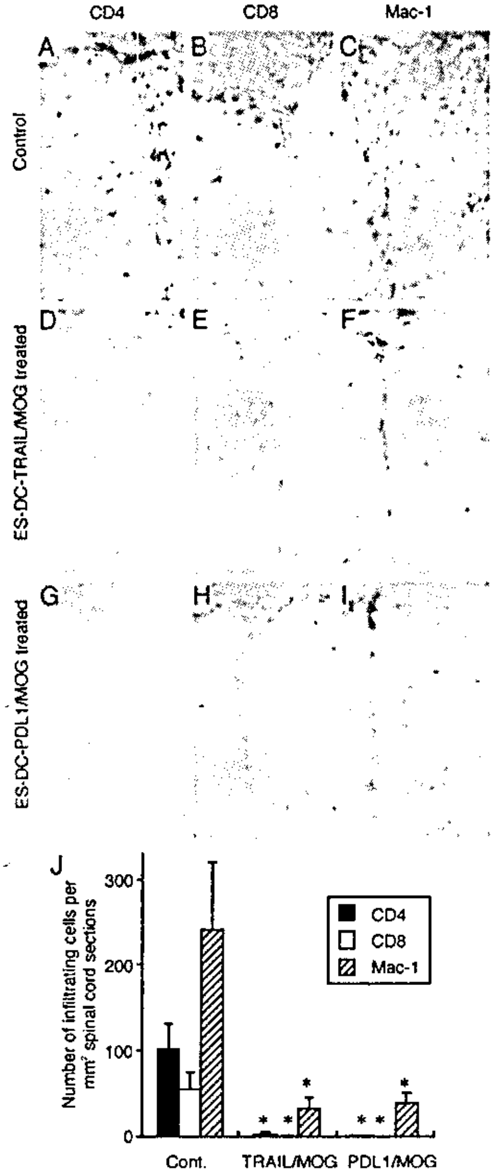

FIGURE 9. Inhibition of infiltration of CD4$^+$ T cells, CD8$^+$ T cells, and Mac-1$^+$ macrophages into spinal cord by treatment of mice with ES-DC expressing MOG plus TRAIL or PD-L1. Mice were pretreated with ES-DC-TRAIL/MOG, PD-L1/MOG, or untreated and subsequently immunized according to the protocol for EAE induction as shown in Fig. 6*A*. The cervical, thoracic, and lumbar spinal cord was isolated at day 11 and subjected to immunohistochemical analysis. CD4 (*A*, *D*, and *G*), CD8 (*B*, *E*, and *H*), and Mac-1 (*C*, *F*, and *I*) staining are shown in representative untreated control (*A–C*), ES-DC-TRAIL/MOG-treated (*D–F*), and ES-DC-PD-L1/MOG-treated (*G–I*) mice. *J*, The positive cells were microscopically counted in three sections of spinal cord. Results are expressed as mean ± SD of CD4$^+$, CD8$^+$, Mac-1$^+$ cells per 1 mm^2 tissue area of samples obtained from five mice. The asterisks indicate that the decreases in number of infiltrated cells are statistically significant ($p < 0.01$) compared with control.

we demonstrated that this methodology worked very effectively for induction of antitumor immunity, showing highly efficient stimulation of Ag-specific T cells by in vivo transfer of ES-DC expressing T cell-attracting chemokines along with Ag (20).

The present study demonstrates the usefulness of the genetically modified DC generated by this method for the treatment of subjects with autoimmune disease. We generated ES-DC presenting the MOG epitope in the context of MHC class II molecule and simultaneously expressing immunosuppressive molecule, TRAIL or PD-L1. By pre- or posttreatment of mice with such ES-DC, we succeeded in preventing an autoimmune disease model, EAE induced by immunization with MOG peptide (Figs. 6 and 7; Table II). Down-modulation of immune response by treatment with genetically modified ES-DC did not affect the immune response to irrelevant exogenous Ag, KLH (Fig. 8*B*). Thus, we achieved the prevention of EAE without decrease in the immune response to an irrelevant Ag.

As for the function of TRAIL, induction of apoptosis has been reported by several groups (3, 4, 42, 44). We also observed an increase in apoptosis of CD4$^+$ T cells in spleens of mice treated with ES-DC-TRAIL/MOG compared with ES-DC-MOG, PD-L1/MOG or RPMI 1640 medium (control), as shown in Fig. 10. The result is consistent with a recent report by Liu et al. (42). They introduced the *TRAIL* gene into bone marrow-derived DC by adenovirus vector and injected the TRAIL transfectant DC into mice for prevention of collagen-induced arthritis, and also observed an increased number of apoptotic T cells in the injected mice. The potential for ES-DC-TRAIL/MOG to cause apoptosis of T cells may have played some role in the protection from EAE, at least in part, in our experiments. In addition, our preliminary experiments suggest that ES-DC-TRAIL/MOG induced T cells with protective

AQ:

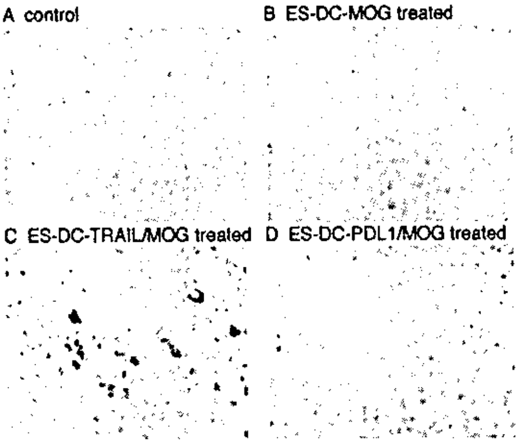

FIGURE 10. Induction of apoptosis of spleen cells by treatment of mice with ES-DC expressing TRAIL along with MOG peptide. Mice were treated with the indicated ES-DC and immunized with MOG peptide, following the schedule described in Fig. 6*A*. On day 11, spleens were isolated from the mice, and apoptotic cells were detected by in situ TUNEL staining. Original magnification, ×200. Sections of the mice untreated (*A*), treated with ES-DC-MOG (*B*), ES-DC-TRAIL/MOG (*C*), and ES-DC-PD-L1/MOG (*D*) are shown. Similar results were observed for three mice used in each experimental group, and representative results are shown.

effects against EAE. In the experiments, we isolated splenic CD4$^+$ T cells from ES-DC-TRAIL/MOG-treated mice and adoptively transferred them to naive mice. The severity of subsequently induced EAE in the recipient mice was significantly reduced by this treatment (data not shown). At present, it may be possible that both induction of apoptosis of MOG-reactive pathogenic T cells and promotion of T cells with some regulatory function contributed to prevention of EAE by ES-DC-TRAIL/MOG. However, to clarify the precise mechanism or character of the T cell with regulatory function, further investigations are necessary.

In contrast, in case of treatment with ES-DC-PDL1/MOG, neither apoptosis of T cells nor induction of transferable disease-preventing T cells was observed (data not shown). We presume induction of anergy of MOG-reactive T cells to be likely as the mechanism of disease-preventive effect of treatment with ES-DC-PD-L1/MOG, based on previous literature regarding the function of PD-L1 (7, 14, 45–47).

To determine whether the profile of cytokine production was altered by treatment with ES-DC, we did ELISA to quantify IL-10, IL-4, and IFN-γ produced by spleen cells of ES-DC-treated mice upon stimulation with MOG peptide in vitro. We observed no significant change in the amount of these cytokines produced by spleen cells from ES-DC-TRAIL/MOG-treated or ES-DC-PDL1/MOG-treated mice, compared with those from ES-DC-MOG-treated mice (data not shown). The level of expression of mRNA for TGF-β detected by RT-PCR was also unchanged compared with control (data not shown). Thus, involvement of IL-10-producing Tr-1 cells or Th2 cells in protection from EAE by treatment with ES-DC-TRAIL/MOG or ES-DC-PD-L1/MOG is unlikely, although one cannot totally rule out the possibility.

The capacity of the ES cells to differentiate to ES-DC was never impaired even after culture for at least over 4 mo. Inactivation of transcription of introduced genes due to gene silencing in ES cells can be prevented using vectors bearing the IRES-drug resistance gene or by targeted gene introduction with an exchangeable gene-trap system (2). Thus, genetically manipulated ES cells can be used as an infinite source for DC with genetically modified properties.

Recently, we established methods for generation of DC from nonhuman primate ES cells and also for genetic modification of them (S. Senju, H. Suemori, H. Matsuyoshi, S. Hirata, Y. Uemura, Y.-Z. Chen, D. Fukuma, M. Furuya, N. Nakatsuji, and Y. Nishimura, manuscript in preparation). We hope to apply this method to human ES cells to generate genetically modified human ES-DC, although some modification might be necessary. In the future, Ag-specific immune modulation therapy by in vivo transfer of human ES-DC expressing antigenic protein along with immune-regulating molecules may well be realized, based on evidence in the current study in the mouse system. Possible applications of this technology are treatment of subjects with autoimmune and allergic diseases and also for induction of tolerance to transplanted organs, especially those generated from ES cells. Thus, the methods established in the present study may have implications as a broad medical technology.

AQ:

Acknowledgments

We thank Dr. S. Aizawa (RIKEN Center for Developmental Biology, Kobe, Japan) for TT2, Drs. N. Takakura (Kanazawa University, Kanazawa, Japan) and T. Suda (Keio University, Tokyo, Japan) for OP9, Dr. H. Niwa (Riken Center for Developmental Biology, Kobe, Japan) for pCAG-IPuro, Drs. T. Okazaki and T. Honjo (Kyoto University, Kyoto, Japan) for a cDNA clone for PD-L1, Tatsuko Kubo (Department of Molecular Pathology, Kumamoto University) for technical assistance, and Kirin Brewery Co., Ltd., for rGM-CSF. M. Ohara (Fukuoka, Japan) provided helpful comments on the manuscript.

References

1. Fujii, S., S. Senju, Y. Z. Chen, M. Ando, S. Matsushita, and Y. Nishimura. 1998. The CLIP-substituted invariant chain efficiently targets an antigenic peptide to HLA class II pathway in L cells. *Hum. Immunol. 59:607.*
2. Senju, S., S. Hirata, H. Matsuyoshi, M. Masuda, Y. Uemura, K. Araki, K. Yamamura, and Y. Nishimura. 2003. Generation and genetic modification of dendritic cells derived from mouse embryonic stem cells. *Blood 101:3501.*
3. Wiley, S. R., K. Schooley, P. J. Smolak, W. S. Din, C. P. Huang, J. K. Nicholl, G. R. Sutherland, T. D. Smith, C. Rauch, C. A. Smith, and R. G. Goodwin. 1995. Identification and characterization of a new member of the TNF family that induces apoptosis. *Immunity 3:673.*
4. Kayagaki, N., N. Yamaguchi, M. Nakayama, K. Takeda, H. Akiba, H. Tsutsui, H. Okamura, K. Nakanishi, K. Okumura, and H. Yagita. 1999. Expression and function of TNF-related apoptosis-inducing ligand on murine activated NK cells. *J. Immunol. 163:1906.*
5. Lamhamedi-Cherradi, S. E., S. J. Zheng, K. A. Maguschak, J. Peschon, and Y. H. Chen. 2003. Defective thymocyte apoptosis and accelerated autoimmune diseases in TRAIL$^{-/-}$ mice. *Nat. Immunol. 4:255.*
6. Dong, H., G. Zhu, K. Tamada, and L. Chen. 1999. B7–H1, a third member of the B7 family, co-stimulates T-cell proliferation and interleukin-10 secretion. *Nat. Med. 5:1365.*
7. Freeman, G. J., A. J. Long, Y. Iwai, K. Bourque, T. Chernova, H. Nishimura, L. J. Fitz, N. Malenkovich, T. Okazaki, M. C. Byrne, et al. 2000. Engagement of the PD-1 immunoinhibitory receptor by a novel B7 family member leads to negative regulation of lymphocyte activation. *J. Exp. Med. 192:1027.*
8. Nishimura, H., M. Nose, H. Hiai, N. Minato, and T. Honjo. 1999. Development of lupus-like autoimmune diseases by disruption of the *PD-1* gene encoding an ITIM motif-carrying immunoreceptor. *Immunity 11:141.*
9. Nishimura, H., T. Okazaki, Y. Tanaka, K. Nakatani, M. Hara, A. Matsumori, S. Sasayama, A. Mizoguchi, H. Hiai, N. Minato, and T. Honjo. 2001. Autoimmune dilated cardiomyopathy in PD-1 receptor-deficient mice. *Science 291:319.*
10. Song, K., Y. Chen, R. Goke, A. Wilmen, C. Seidel, A. Goke, and B. Hilliard. 2000. Tumor necrosis factor-related apoptosis-inducing ligand (TRAIL) is an inhibitor of autoimmune inflammation and cell cycle progression. *J. Exp. Med. 191:1095.*
11. Hilliard, B., A. Wilmen, C. Seidel, T. S. Liu, R. Goke, and Y. Chen. 2001. Roles of TNF-related apoptosis-inducing ligand in experimental autoimmune encephalomyelitis. *J. Immunol. 166:1314.*
12. Lunemann, J. D., S. Waiczies, S. Ehrlich, U. Wendling, B. Seeger, T. Kamradt, and F. Zipp. 2002. Death ligand TRAIL induces no apoptosis but inhibits activation of human (auto)antigen-specific T cells. *J. Immunol. 168:4881.*
13. Kayagaki, N., N. Yamaguchi, M. Abe, S. Hirose, T. Shirai, K. Okumura, and H. Yagita. 2002. Suppression of antibody production by TNF-related apoptosis-inducing ligand (TRAIL). *Cell. Immunol. 219:82.*
14. Nishimura, H., and T. Honjo. 2001. PD-1: an inhibitory immunoreceptor involved in peripheral tolerance. *Trends Immunol. 22:265.*
15. Okazaki, T., Y. Iwai, and T. Honjo. 2002. New regulatory co-receptors: inducible co-stimulator and PD-1. *Curr. Opin. Immunol. 14:779.*
16. Salama, A. D., T. Chitnis, J. Imitola, M. J. Ansari, H. Akiba, F. Tushima, M. Azuma, H. Yagita, M. H. Sayegh, and S. J. Khoury. 2003. Critical role of the

programmed death-1 (PD-1) pathway in regulation of experimental autoimmune encephalomyelitis. *J. Exp. Med. 198:71.*

17. Liang, S. C., Y. E. Latchman, J. E. Buhlmann, M. F. Tomczak, B. H. Horwitz, G. J. Freeman, and A. H. Sharpe. 2003. Regulation of PD-1, PD-L1, and PD-L2 expression during normal and autoimmune responses. *Eur. J. Immunol. 33:2706.*
18. Ansari, M. J., A. D. Salama, T. Chitnis, R. N. Smith, H. Yagita, H. Akiba, T. Yamazaki, M. Azuma, H. Iwai, S. J. Khoury, et al. 2003. The programmed death-1 (PD-1) pathway regulates autoimmune diabetes in nonobese diabetic (NOD) mice. *J. Exp. Med. 198:63.*
19. Fairchild, P. J., F. A. Brook, R. L. Gardner, L. Graca, V. Strong, Y. Tone, M. Tone, K. F. Nolan, and H. Waldmann. 2000. Directed differentiation of dendritic cells from mouse embryonic stem cells. *Curr. Biol. 10:1515.*
20. Matsuyoshi, H., S. Senju, S. Hirata, Y. Yoshitake, Y. Uemura, and Y. Nishimura. 2004. Enhanced priming of antigen-specific CTLs in vivo by embryonic stem cell-derived dendritic cells expressing chemokine along with antigenic protein: application to antitumor vaccination. *J. Immunol. 172:776.*
21. Fairchild, P. J., K. F. Nolan, S. Cartland, L. Graca, and H. Waldmann. 2003. Stable lines of genetically modified dendritic cells from mouse embryonic stem cells. *Transplantation 76:606.*
22. Cheng, P., Y. Nefedova, L. Miele, B. A. Osborne, and D. Gabrilovich. 2003. Notch signaling is necessary but not sufficient for differentiation of dendritic cells. *Blood 102:3980.*
23. Mendel, I., N. Kerlero de Rosbo, and A. Ben-Nun. 1995. A myelin oligodendrocyte glycoprotein peptide induces typical chronic experimental autoimmune encephalomyelitis in $H\text{-}2^b$ mice: fine specificity and T cell receptor $V\beta$ expression of encephalitogenic T cells. *Eur. J. Immunol. 25:1951.*
24. Greer, J. M., R. A. Sobel, A. Sette, S. Southwood, M. B. Lees, and V. K. Kuchroo. 1996. Immunogenic and encephalitogenic epitope clusters of myelin proteolipid protein. *J. Immunol. 156:371.*
25. Zamvil, S. S., D. J. Mitchell, M. B. Powell, K. Sakai, J. B. Rothbard, and L. Steinman. 1988. Multiple discrete encephalitogenic epitopes of the autoantigen myelin basic protein include a determinant for I-E class II-restricted T cells. *J. Exp. Med. 168:1181.*
26. Senju, S., K. Iyama, H. Kudo, S. Aizawa, and Y. Nishimura. 2000. Immunocytochemical analyses and targeted gene disruption of GTPBP1. *Mol. Cell. Biol. 20:6195.*
27. Fujii, S., Y. Uemura, L. K. Iwai, M. Ando, S. Senju, and Y. Nishimura. 2001. Establishment of an expression cloning system for $CD4^+$ T cell epitopes. *Biochem. Biophys. Res. Commun. 284:1140.*
28. Uemura, Y., S. Senju, K. Maenaka, L. K. Iwai, S. Fujii, H. Tabata, H. Tsukamoto, S. Hirata, Y. Z. Chen, and Y. Nishimura. 2003. Systematic analysis of the combinatorial nature of epitopes recognized by TCR leads to identification of mimicry epitopes for glutamic acid decarboxylase 65-specific TCRs. *J. Immunol. 170:947.*
29. Weir, C. R., K. Nicolson, and B. T. Backstrom. 2002. Experimental autoimmune encephalomyelitis induction in naive mice by dendritic cells presenting a self-peptide. *Immunol. Cell Biol. 80:14.*
30. Legge, K. L., R. K. Gregg, R. Maldonado-Lopez, L. Li, J. C. Caprio, M. Moser, and H. Zaghouani. 2002. On the role of dendritic cells in peripheral T cell tolerance and modulation of autoimmunity. *J. Exp. Med. 196:217.*
31. Bonham, C. A., L. Lu, R. A. Banas, P. Fontes, A. S. Rao, T. E. Starzl, A. Zeevi, and A. W. Thomson. 1996. TGF-β1 pretreatment impairs the allostimulatory function of human bone marrow-derived antigen-presenting cells for both naive and primed T cells. *Transpl. Immunol. 4:186.*
32. Lutz, M. B., R. M. Suri, M. Niimi, A. L. Ogilvie, N. A. Kukutsch, S. Rossner, G. Schuler, and J. M. Austyn. 2000. Immature dendritic cells generated with low doses of GM-CSF in the absence of IL-4 are maturation resistant and prolong allograft survival in vivo. *Eur. J. Immunol. 30:1813.*
33. Steinbrink, K., M. Wolfl, H. Jonuleit, J. Knop, and A. H. Enk. 1997. Induction of tolerance by IL-10-treated dendritic cells. *J. Immunol. 159:4772.*
34. Menges, M., S. Rossner, C. Voigtlander, H. Schindler, N. A. Kukutsch, C. Bogdan, K. Erb, G. Schuler, and M. B. Lutz. 2002. Repetitive injections of dendritic cells matured with tumor necrosis factor-α induce antigen-specific protection of mice from autoimmunity. *J. Exp. Med. 195:15.*
35. Sato, K., N. Yamashita, M. Baba, and T. Matsuyama. 2003. Regulatory dendritic cells protect mice from murine acute graft-versus-host disease and leukemia relapse. *Immunity 18:367.*
36. Sato, K., N. Yamashita, M. Baba, and T. Matsuyama. 2003. Modified myeloid dendritic cells act as regulatory dendritic cells to induce anergic and regulatory T cells. *Blood 101:3581.*
37. Dhodapkar, M. V., R. M. Steinman, J. Krasovsky, C. Munz, and N. Bhardwaj. 2001. Antigen-specific inhibition of effector T cell function in humans after injection of immature dendritic cells. *J. Exp. Med. 193:233.*
38. Takayama, T., Y. Nishioka, L. Lu, M. T. Lotze, H. Tahara, and A. W. Thomson. 1998. Retroviral delivery of viral interleukin-10 into myeloid dendritic cells markedly inhibits their allostimulatory activity and promotes the induction of T-cell hyporesponsiveness. *Transplantation 66:1567.*
39. Lu, L., A. Gambotto, W. C. Lee, S. Qian, C. A. Bonham, P. D. Robbins, and A. W. Thomson. 1999. Adenoviral delivery of CTLA4Ig into myeloid dendritic cells promotes their in vitro tolerogenicity and survival in allogeneic recipients. *Gene Ther. 6:554.*
40. Min, W. P., R. Gorczynski, X. Y. Huang, M. Kushida, P. Kim, M. Obataki, J. Lei, R. M. Suri, and M. S. Cattral. 2000. Dendritic cells genetically engineered to express Fas ligand induce donor-specific hyporesponsiveness and prolong allograft survival. *J. Immunol. 164:161.*
41. Terness, P., T. M. Bauer, L. Rose, C. Dufter, A. Watzlik, H. Simon, and G. Opelz. 2002. Inhibition of allogeneic T cell proliferation by indoleamine 2,3-dioxygenase-expressing dendritic cells: mediation of suppression by tryptophan metabolites. *J. Exp. Med. 196:447.*
42. Liu, Z., X. Xu, H. C. Hsu, A. Tousson, P. A. Yang, Q. Wu, C. Liu, S. Yu, H. G. Zhang, and J. D. Mountz. 2003. CII-DC-AdTRAIL cell gene therapy inhibits infiltration of CII-reactive T cells and CII-induced arthritis. *J. Clin. Invest. 112:1332.*
43. Morita, Y., J. Yang, R. Gupta, K. Shimizu, E. A. Shelden, J. Endres, J. J. Mule, K. T. McDonagh, and D. A. Fox. 2001. Dendritic cells genetically engineered to express IL-4 inhibit murine collagen-induced arthritis. *J. Clin. Invest. 107:1275.*
44. Giovarelli, M., P. Musiani, G. Garotta, R. Ebner, E. Di Carlo, Y. Kim, P. Cappello, L. Rigamonti, P, Bernabei, F. Novelli, et al. 1999. A "stealth effect": adenocarcinoma cells engineered to express TRAIL elude tumor-specific and allogeneic T cell reactions. *J. Immunol. 163:4886.*
45. Brown, J. A., D. M. Dorfman, F. R. Ma, E. L. Sullivan, O. Munoz, C. R. Wood, E. A. Greenfield, and G. J. Freeman. 2003. Blockade of programmed death-1 ligands on dendritic cells enhances T cell activation and cytokine production. *J. Immunol. 170:1257.*
46. Carter, L., L. A. Fouser, J. Jussif, L. Fitz, B. Deng, C. R. Wood, M. Collins, T. Honjo, G. J. Freeman, and B. M. Carreno. 2002. PD-1:PD-L inhibitory pathway affects both $CD4^+$ and $CD8^+$ T cells and is overcome by IL-2. *Eur. J. Immunol. 32:634.*
47. Selenko-Gebauer, N., O. Majdic, A. Szekeres, G. Hofler, E. Guthann, U. Korthauer, G. Zlabinger, P. Steinberger, W. F. Pickl, H. Stockinger, et al. 2003. B7-H1 (programmed death-1 ligand) on dendritic cells is involved in the induction and maintenance of T cell anergy. *J. Immunol. 170:3637.* AQ:

THE JOURNAL OF BIOLOGICAL CHEMISTRY
© 2004 by The American Society for Biochemistry and Molecular Biology, Inc.

Vol. 279, No. 46, Issue of November 12, pp. 48457–48465, 2004
Printed in U.S.A.

B-Raf Contributes to Sustained Extracellular Signal-regulated Kinase Activation Associated with Interleukin-2 Production Stimulated through the T Cell Receptor*

Received for publication, March 19, 2004, and in revised form, August 27, 2004
Published, JBC Papers in Press, August 31, 2004, DOI 10.1074/jbc.M403087200

Hirotake Tsukamoto, Atsushi Irie, and Yasuharu Nishimura‡

From the Department of Immunogenetics, Graduate School of Medical Sciences, Kumamoto University, Honjo 1-1-1, Kumamoto 860-8556, Japan

A T cell receptor (TCR) recognizes and responds to an antigenic peptide in the context of major histocompatibility complex-encoded molecules. This provokes T cells to produce interleukin-2 (IL-2) through extracellular signal-regulated kinase (ERK) activation. We investigated the roles of B-Raf in TCR-mediated IL-2 production coupled with ERK activation in the Jurkat human T cell line. We found that TCR cross-linking could induce up-regulation of both B-Raf and Raf-1 activities, but Raf-1 activity was decreased rapidly. On the other hand, TCR-stimulated kinase activity of B-Raf was sustained. Expression of a dominant-negative mutant of B-Raf abrogated sustained but not transient TCR-mediated MEK/ERK activation. The inhibition of sustained ERK activation by either expression of a dominant-negative B-Raf or treatment with a MEK inhibitor resulted in a decrease of the TCR-stimulated nuclear factor of activated T cells (NFAT) activity and IL-2 production. Collectively, our data provide the first direct evidence that B-Raf is a positive regulator of TCR-mediated sustained ERK activation, which is required for NFAT activation and the full production of IL-2.

T cells recognize self or non-self peptides in the context of major histocompatibility complex (MHC)[1]-encoded molecules via T cell receptors (TCRs), and the signals are then transduced into the nucleus. These signals determine the fate of T cells and induce cytokine production, cytolytic activity, survival, apoptosis, and proliferation (1). Within seconds of MHC-peptide engagement, TCR components initiate phosphorylation cascades that trigger multiple branching signaling pathways. One well studied key switch is the activation signal of extracellular signal-regulated kinase 1/2 (ERK1/2), which is mediated by the small GTP-binding proteins, Ras (2, 3) and Rap1 (4, 5). Current models suggest that TCR stimulation with the agonistic peptide-MHC complex activates the conversion of Ras from the GDP- to GTP-bound form (2, 6). Activated Ras subsequently recruits the serine/threonine kinase Raf-1 to the plasma membrane, resulting in its activation. Activated Raf-1 then activates ERK kinase (MEK), which directly phosphorylates tyrosine and threonine residues (TEY motif) on ERK1/2 to activate them (6). These signals combine to activate multiple transcription factors, including nuclear factor of activated T cells (NFAT), NF-κB, and activating protein-1 (AP-1), all of which contribute toward the production of IL-2 (7–9).

ERK1/2 are involved in a diverse array of cellular functions including cell growth and apoptosis of T cells (10–12). In ERK1-deficient mice, the thymocyte differentiation from $CD4^+CD8^+$ double positive to the $CD4^+/CD8^+$ single positive stage is impaired; thus, ERK activation by TCR ligation plays important roles in T cell development (13). Experiments using pharmacological inhibitors of MEK and dominant negative MEK also provided evidence that ERK1/2 are critical for thymocyte differentiation (11, 14) and for induction of TCR-mediated mitogenic signals and IL-2 production in mature T cells (7, 15). Hence, it is important to understand how the strength and duration of ERK activity is regulated in TCR-mediated activation and fate decisions of T cells.

The functions of ERK signaling are regulated by its upstream elements, in particular by members of the Raf family, in various cell types, and three Raf isoforms, Raf-1, A-Raf, and B-Raf, are expressed in mammalian cells (16, 17). Whereas Raf-1 is ubiquitously expressed, B-Raf shows a more restricted expression pattern (18, 19). Mice deficient in the different Raf isoforms exhibit different developmental defects, suggesting the nonredundant function(s) of each Raf isoform (20). A different phenotype of each Raf-deficient mouse is expected to be due, at least in part, to their distinct expression pattern. It was reported that B-Raf exhibits a much more basal kinase activity and a higher affinity toward MEK than does Raf-1 *in vitro* (21). Despite these differences, the specific function(s) *in vivo*, if any, of each Raf isoform is poorly understood. B-Raf was reported to be one component of the receptor-mediated MEK/ERK activation pathway in fibroblasts, B cell lines, and PC12 cells (21–26). Moreover, B-Raf expression in T cells is controversial; in this study, we detected B-Raf protein in Jurkat cells and primary human T cells, whereas others did not (4).

Although Raf-1 is a well characterized effector molecule for ERK activation in the TCR-mediated signaling cascade and IL-2 production in T cells (27), much less attention has been directed to the roles of B-Raf in T cells. We now report that interaction of B-Raf with MEK and B-Raf activity are induced in a TCR stimulation-dependent manner in Jurkat cells. Our data suggest that MEK/ERK activity are selectively regulated through the Ras/B-Raf signaling pathway and that the sustained B-Raf/MEK/ERK activation is indispensable for the

---

* This work was supported in part by Grants-in-Aid 12051203, 14370115, and 15510165 from the Ministry of Education, Science, Technology, Sports, and Culture, Japan. The costs of publication of this article were defrayed in part by the payment of page charges. This article must therefore be hereby marked "*advertisement*" in accordance with 18 U.S.C. Section 1734 solely to indicate this fact.

‡ To whom correspondence should be addressed: Dept. of Immunogenetics, Graduate School of Medical Sciences, Kumamoto University, Honjo 1-1-1, Kumamoto 860-8556, Japan. Tel.: 81-96-373-5310; Fax: 81-96-373-5314; E-mail: mxnishim@gpo.kumamoto-u.ac.jp.

[1] The abbreviations used are: MHC, major histocompatibility complex; AP-1, activating protein-1; ERK, extracellular signal-regulated kinase; GST, glutathione *S*-transferase; HA, hemagglutinin; IL-2, interleukin-2; MEK, mitogen-activated protein kinase/ERK kinase; NFAT, nuclear factor of activated T cells; TCR, T cell receptor; GFP, green fluorescent protein.

This paper is available on line at http://www.jbc.org

translocation of NFAT into the nucleus and for the production of IL-2.

EXPERIMENTAL PROCEDURES

Cell Preparations and Reagents—Jurkat cell clone, E6-1 from the American Type Culture Collection, and Jurkat cells expressing simian virus 40 large T antigen (TAg-Jurkat) (28) were maintained in RPMI 1640 medium (RPMI) supplemented with 10% fetal calf serum, 2 mM L-glutamine, and penicillin/streptomycin (100 units/ml and 100 μg/ml, respectively). Jurkat cells stably expressing a wild-type or a dominant negative form of B-Raf were established and maintained in RPMI plus 10% fetal calf serum with 2 mg/ml G418. The human CD4$^+$ T cell clone, YN 5–32 and peripheral blood mononuclear cells were prepared as described (29, 30). For transient and stable transfection, 2×10^7 Jurkat cells were resuspended in 500 μl of cytomix (31) with the appropriate cDNAs. The amount of plasmid DNA was held at 40 μg constant by the addition of the pcDNA3 vector control. Cells were electroporated in 310 V at a capacitance of 960 microfarads. Transfectants were analyzed for CD3 and CD28 expression using flow cytometry (BD Biosciences). Anti-CD3 (clone UCHT-1) antibody, anti-CD28 (clone L923) antibody, and rabbit polyclonal anti-GFP antibody were purchased from Pharmingen. Anti-mouse IgG (Fab-specific) antibody was from Sigma. Mouse monoclonal anti-NFAT1 and anti-NFAT2 antibodies and rabbit polyclonal antibodies specific to Raf-1, B-Raf, MEK-1, c-Fos, and Lamin B were purchased from Santa Cruz Biotechnology, Inc. (Santa Cruz, CA). Polyclonal antibodies specific to MEK, phospho-ERK, phospho-p38, and phospho-MEK and a MEK inhibitor, U0126, were purchased from New England Biolabs (Beverly, MA). Mouse monoclonal anti-hemagglutinin (HA) antibody was from Covance (Berkeley, CA). Cy3-labeled anti-rabbit Ig antibody, horseradish peroxidase-conjugated rabbit anti-mouse IgG, and donkey anti-rabbit IgG were from Amersham Biosciences. Anti-human IL-2 antibodies were from R & D Systems (Minneapolis, MN). Recombinant glutathione *S*-transferase (GST)-MEK was prepared as reported (32).

The pcDNA3 expression vectors with HA-tagged wild-type and dominant negative mutant B-Raf cDNAs were provided by Dr. K. L. Guan (33). The RasN17 expression vector was a gift from Dr. T. Kinashi (5). The luciferase reporter construct for IL-2 promoter and AP-1 binding site were kindly provided by Dr. V. A. Boussiotis (34) and Dr. R. M. Niles (35), respectively. The expression vector for GST-MEK was a gift from Dr. Y. Takai (32). NFAT-green fluorescence protein (GFP) reporter construct, consisting of three tandem NFAT-binding sites followed by a gene encoding GFP, was provided by Dr. T. Saito (36).

Cell Stimulation and Inhibitor Treatment—In experiments for stimulation with soluble anti-CD3 antibody for cross-linking, Jurkat cells were incubated on ice for 20 min and then incubated with anti-CD3 antibody (0.25 μg/ml) for 10 min followed by the addition of anti-mouse IgG antibody (1 μg/ml) for 5 min. After the indicated times of incubation at 37 °C, cells were harvested and lysed with lysis buffer (see below). For the analysis of promoter activity and IL-2 production, Jurkat cells (1×10^6/well) were stimulated with immobilized anti-CD3 and CD28 antibodies (5 and 10 μg/ml, respectively). For experiments with inhibitor treatment, cells were preincubated for 30 min with the MEK inhibitor U0126 or Me_2SO as a control. In the time course analyses of the effect of ERK activation on IL-2 production by the treatment with U0126, medium containing U0126 or Me_2SO was added at the indicated time points.

Western Blotting, Immunoprecipitation, and in Vitro Kinase Assay—After the indicated times of stimulation, the Jurkat cells were recovered and lysed with lysis buffer (1% Nonidet P-40, 150 mM NaCl, 50 mM Tris, pH 7.4, 1 mM EDTA, 0.25% sodium deoxycholate, a protease inhibitor tablet (Roche Applied Science)). SDS-PAGE, Western blotting, and immunoprecipitations from the cell lysates were carried out as described (30). Raf-1 and B-Raf were immunoprecipitated from cell lysates of T cells with the anti-Raf-1 and the anti-B-Raf antibodies, respectively, as described above. The immunoprecipitates were resuspended in 25 mM HEPES (pH 7.5), 10 mM $MgCl_2$, 10 mM β-glycerophosphate, 1 mM dithiothreitol, 10 μCi of [γ-^{32}P]ATP (Amersham Biosciences), and 0.8 μg of recombinant GST-MEK protein. Reaction mixtures were incubated at 32 °C for 20 min, and then the reactions were terminated by adding 5× SDS sample buffer, separated on 7% SDS-PAGE under the reducing condition, transferred to nitrocellulose membrane, and exposed to x-ray film. Relative amounts of MEK or ERK phosphorylation were calculated based on the ratio of the intensities of phospho-MEK or phospho-ERK bands to those of the whole MEK or ERK bands in whole cell lysates at each time point. Signal intensities of the bands were quantified by densitometric analysis using NIH Image 6.2 software. Nuclear extracts were prepared from B-Raf mutant- or mock-transfected TAg Jurkat cells for nuclear translocation analysis of NFAT using nuclear/cytosol fractionation kits (BioVision).

Flow Cytometric Analysis and Cytokine Measurement—For the NFAT-GFP reporter assay, the TAg-Jurkat cells expressing B-Raf AA or mock vector were transfected with NFAT-GFP reporter construct and stimulated for 9 h with immobilized anti-CD3 and anti-CD28 antibodies. The expression of GFP was analyzed with a flow cytometer and CellQuest software (BD Biosciences). For intracellular staining, cells were fixed and permeabilized with IntraPrep (Immunotech, Marseille, France) and then stained with appropriate fluorescence-labeled antibodies. IL-2 concentrations in supernatants of T cell culture after 48 h of stimulation were measured in an enzyme-linked immunosorbent assay using anti-human IL-2 antibodies.

Reverse Transcription-PCR—Total RNA extraction and first-strand cDNA synthesis from T cells were done as described (37). The cDNA was subjected to PCR amplification using a set of primers specific for human *B-Raf*: 5′-ACAACAGTTATTGGAATCTCTGG-3′ and 5′-AAATGCTAAGGTGAAAAACG-3′.

Luciferase Assay—Reporter constructs were transfected into the Jurkat cells expressing wild-type or mutant B-Raf. A β-galactosidase expression plasmid was co-transfected to normalize the variations in transfection efficiency. After 12 h of transfection, cells were harvested and stimulated. Luciferase assay was carried out according to the protocol in the Pica Gene kit (Toyo Ink, Tokyo, Japan). β-Galactosidase expression was assessed using the Luminescent β-galactosidase detection kit II (Clontech) according to the manufacturer's instructions.

RESULTS

Expression of B-Raf Proteins in Both Human and Mouse T Cells—We investigated the expression of B-Raf in human and mouse T cells using Western blotting (Fig. 1*A*). Rat PC12 cells, as a positive control gave a 95-kDa band corresponding to B-Raf (*lane 1*), whereas B-Raf expression was negligible in NIH3T3 cells, as reported (*lane 2*) (38). B-Raf was detected in a human CD4$^+$ T cell clone, YN5–32 (*lane 3*) (29, 30), a human T cell line, Jurkat (*lane 4*), and mouse CD4$^+$ T cells isolated from spleens (*lanes 5*). Furthermore, the expression of human B-Raf mRNA was assessed by reverse transcription-PCR using RNAs isolated from the YN5–32 T cell clone and from Jurkat T cells (data not shown). Intracellular staining and flow cytometric analysis also confirmed the B-Raf expression in human CD3-positive peripheral T cells (Fig. 1*B*) and mouse TCR-β chain-positive splenic T cells (Fig. 1*B*, *b*). Taken together, we conclude that B-Raf is expressed in both human and mouse T cells, allowing us to examine B-Raf functions in TCR-mediated T cell activation.

TCR Ligation Induces Both Raf-1 and B-Raf Activation—Cross-linking of TCRs with soluble anti-CD3 antibody, which mimics the engagement of TCR with the agonistic peptide-MHC complex, induced ERK and MEK phosphorylation within 1 min, reaching a maximal level at ~1–3 min in Jurkat cells (Fig. 2*A*). The ERK/MEK phosphorylations displayed similar kinetics and were prolonged for up to 60 min. Next, we performed *in vitro* kinase assays for Raf-1 and B-Raf to estimate the strength and kinetics of their kinase activities. Consistent with the previous report (27), Raf-1 was activated at 3 min after TCR ligation and became inactive within 20 min (Fig. 2*B*). In contrast to the kinetics of Raf-1 activity, there was slight but detectable B-Raf activity even under the basal condition, and B-Raf showed a pronounced increase of its kinase activity at 3 min after TCR stimulation. B-Raf kinase activity was gradually decreased but did last for up to 60 min (Fig. 2*B*). Raf-1 was inactivated after 20 min of TCR ligation; nevertheless, apparent MEK/ERK activation was still sustained up to 60 min (Fig. 2*A*). Intriguingly, the kinetics of TCR-mediated B-Raf activation rather than that of Raf-1 activation was similar to that of MEK/ERK activation. The addition of co-stimulation with an anti-CD28 antibody treatment slightly enhanced the B-Raf activity over time compared with that stimulated with an anti-CD3 antibody alone (Fig. 2*C*).

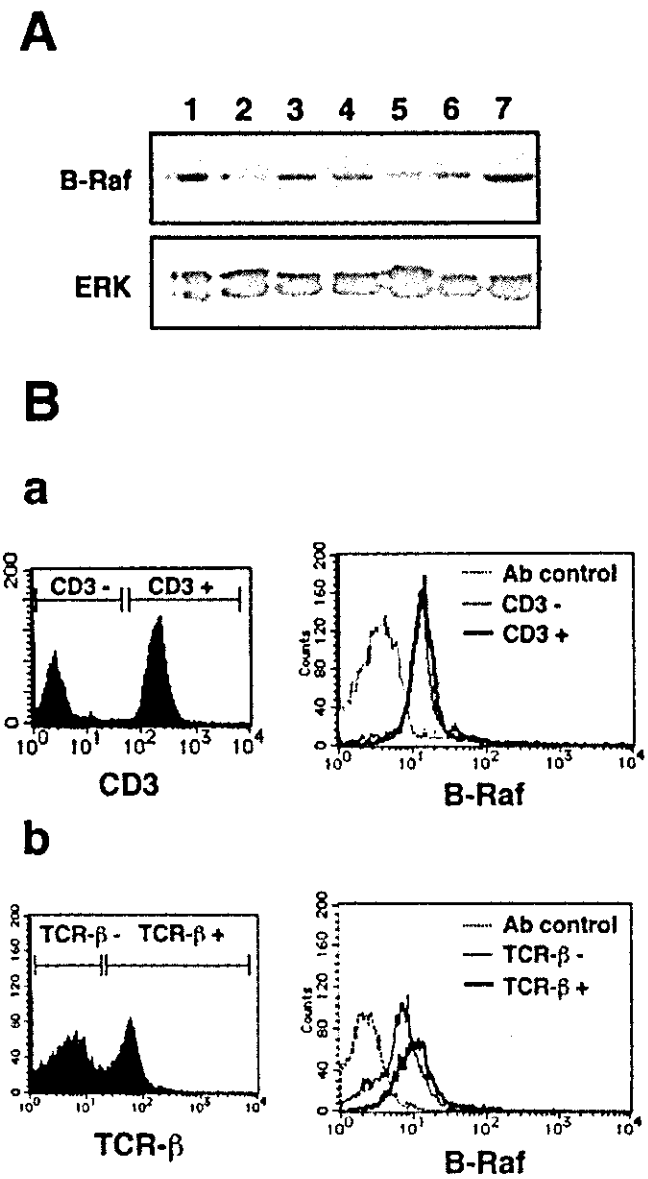

FIG. 1. **B-Raf is expressed in both human and mouse T cells.** *A*, Western blotting analysis using an anti-B-Raf antibody (*top panel*). *Lane 1*, PC12 cells; *lane 2*, NIH3T3 cells; *lane 3*, human CD4⁺ T cell clone, YN5–32; *lane 4*, Jurkat cells; *lane 5*, mouse CD4⁺ T cells isolated from spleen; *lane 6*, HeLa cells; *lane 7*, HeLa cells transfected with B-Raf. ERK blotting indicates comparable protein loading (*bottom panel*). *B*, flow cytometric analyses of B-Raf expression. Human peripheral blood mononuclear cells were stained with an anti-CD3 antibody (*a*) and murine spleen cells were stained with anti-mouse TCR-β chain antibody (*b*) (*left panels*). The CD3 or TCR-β chain negative and positive cell populations were gated, and intracellular B-Raf staining was carried out (*right panels*). An irrelevant rabbit polyclonal antibody was used as negative control for staining. *Ab*, antibody.

Physiological association between Raf family kinases and MEK is necessary for MEK/ERK activation (39); hence, we asked if B-Raf can interact with MEK in T cells in response to TCR stimulation using co-immunoprecipitation methods. For this purpose, wild-type B-Raf tagged with HA was expressed in Jurkat cells and was immunoprecipitated with an anti-HA antibody. The specific association between HA-B-Raf and MEK was achieved at a maximal level at 3 min after TCR ligation, and this interaction lasted for up to 60 min with a slight decrease (Fig. 2*D*). The intrinsic interaction between B-Raf and MEK was also evaluated by reciprocal immunoprecipitation experiments using an anti-MEK antibody to detect endogenous B-Raf protein. As shown in Fig. 2*E*, endogenous B-Raf protein was not detected in immunoprecipitates with the anti-MEK antibody in unstimulated Jurkat cells. Consistent with Fig. 2*D*, intrinsic B-Raf·MEK complex formation was strongly induced at 3 min after TCR ligation, and then it decreased gradually but remained above the basal level up to 60 min after TCR stimulation *in vivo* (Fig. 2*E*). The kinetics of B-Raf/MEK interaction paralleled those of B-Raf activation (Fig. 2*B*). These results strongly suggested that B-Raf was involved in MEK/ERK activation stimulated with TCR ligation, especially in the late phase after Raf-1 had become inactive (Fig. 2*B*).

TCR-mediated B-Raf Activation Is Partly Dependent on Ras Activity—Previous studies reported that B-Raf activation in fibroblasts was dependent on Ras activation (40, 41). In other cases, Ras activity was not essential for B-Raf activation in PC12 cells (23, 38). In T cells, to determine whether Ras activity is required for the B-Raf activation, TCR-mediated B-Raf activity was measured in TAg-Jurkat expressing the dominant negative Ras mutant RasN17. The RasN17 interfered with endogenous Ras, Raf-1, and MEK/ERK activation until at least 60 min after TCR stimulation (data not shown) (2). As shown in Fig. 3, TCR engagement resulted in a robust activation of B-Raf after stimulation in mock-transfected Jurkat cells. In contrast, RasN17-transfected cells showed decreased B-Raf activation as compared with that observed in the control cells at 3 min after TCR stimulation (75% reduction). Similar inhibitory effects was observed at any given time points. These results indicated that TCR-mediated B-Raf activation is, at least in part, regulated by Ras activation *in vivo*.

B-Raf Contributes to Sustained MEK/ERK Activation—Within the activation segment of B-Raf, there are two sites, Thr^{598} and Ser^{601}, that can be phosphorylated in response to Ras activation, and the phosphorylation status of these residues is required for the maximal kinase activity of B-Raf (33, 40). Hence, we introduced a dominant negative mutant of B-Raf (B-Raf AA), in which Thr^{598} and Ser^{601} were substituted to Ala (33), into T cells to examine the role of B-Raf in TCR-mediated MEK/ERK activation cascade. As shown in Fig. 4*A*, a Jurkat clone expressing B-Raf AA showed a similar degree of MEK/ERK activation induced by TCR cross-linking with soluble anti-CD3 antibody at 3 min after stimulation in comparison with that of mock-transfected cells. The MEK/ERK activation was effectively sustained for 60 min in the mock transfectants. On the other hand, in the Jurkat clone expressing B-Raf AA, MEK/ERK activation returned to the basal level within 30 min after TCR stimulation, and then it was no longer detected. Densitometric analyses of MEK/ERK activation revealed that the activation kinetic pattern rather than the relative magnitude of MEK/ERK activation was distinct between the mock-transfected clone and the B-Raf AA-expressing clone (Fig. 4*B*). Since TAg-Jurkat cells transiently transfected with B-Raf AA showed an essentially similar response, the possibility that these results were specific for one particular clone (AA2) was excluded (Fig. 4*C*). Moreover, these results were not due to the inhibition of Raf-1 activity by B-Raf AA, because the degree of TCR-mediated Raf-1 activation in B-Raf AA-expressing Jurkat cells was indistinguishable from that of mock-transfected Jurkat cells or cells expressing HA-tagged wild-type B-Raf (Fig. 4*D* and data not shown). In contrast to MEK/ERK activation, no significant differences in phosphorylation of another mitogen-activated protein kinase, p38, were detectable in both mock- and B-Raf AA-transfected TAg-Jurkat cells, suggesting that B-Raf AA did not influence p38 activation (Fig. 4*C*). The data indicate that B-Raf physiologically and specifically regulated prolonged MEK/ERK activation induced by TCR stimulation in Jurkat cells.

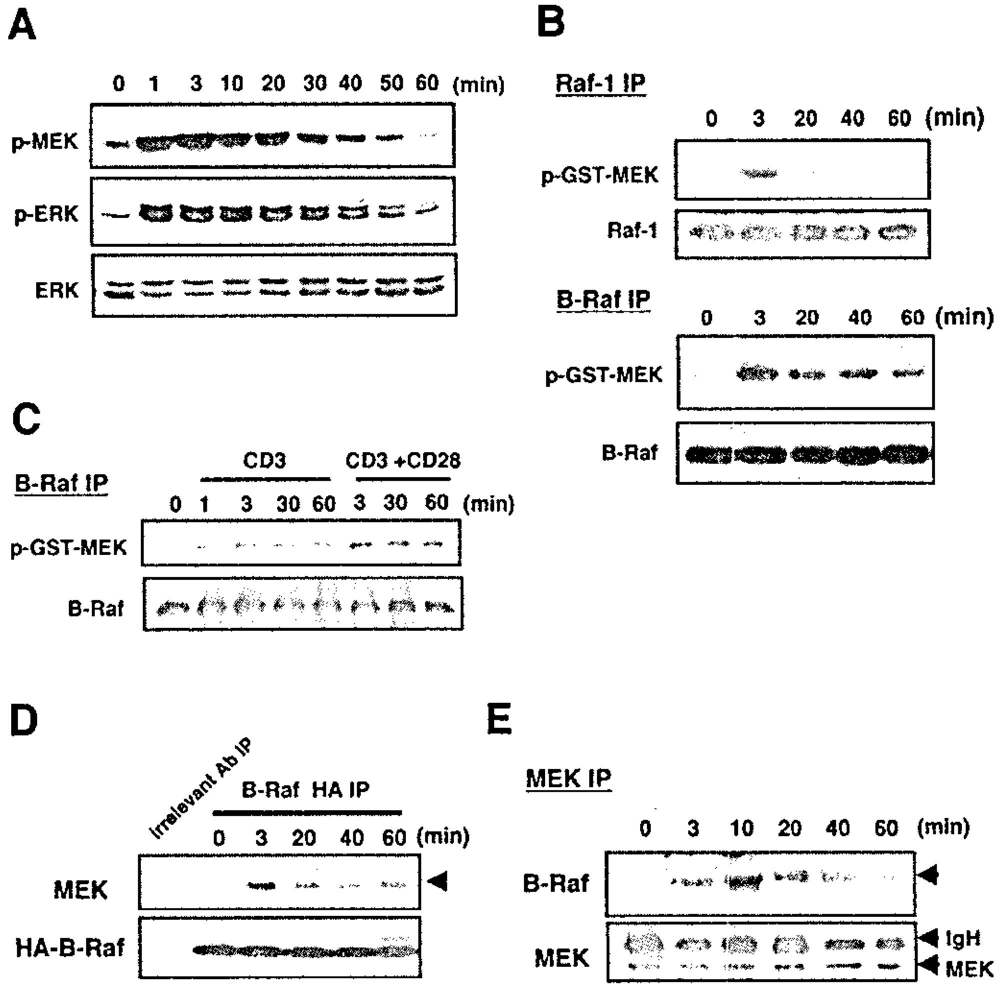

FIG. 2. **B-Raf activation and B-Raf/MEK interaction were induced in a TCR stimulation-dependent manner.** *A*, Jurkat T cells were incubated with or without (0 min) a soluble anti-CD3 antibody together with a second antibody for the indicated times. The cells were subjected to Western blotting with an anti-phospho-MEK-specific antibody (*top panel*) or an anti-phospho-ERK-specific antibody (*middle panel*). Equal protein loading was confirmed by total ERK blotting (*bottom panel*). *B*, *in vitro* kinase assays for Raf-1 and B-Raf isolated from Jurkat cells stimulated with the anti-CD3 antibody for the indicated times. Recombinant GST-MEK was used as a substrate, and incorporated ^{32}P radioactivities were visualized by autoradiography. Equal loading of each Raf protein was confirmed by blotting with either an anti-Raf-1 antibody (*upper bottom panel*) or an anti-B-Raf antibody (*lower bottom panel*). *C*, additive anti-CD28 antibody stimulation enhanced the B-Raf kinase activity. Jurkat cells were stimulated with the anti-CD3 antibody alone or the anti-CD3 together with the anti-CD28 antibodies for the indicated times, and an *in vitro* kinase assay was performed. *D*, TAg-Jurkat cells transiently expressing HA-tagged wild-type B-Raf were stimulated with cross-linking of soluble anti-CD3 antibody for the indicated times. Immunoprecipitates with an anti-HA antibody were blotted with an anti-MEK (*upper panel*) or the anti-HA antibodies (*lower panel*). The immunoprecipitates with irrelevant rabbit IgG in Jurkat cells stimulated for 3 min was used as a negative control. *E*, immunoprecipitates with an anti-MEK antibody from Jurkat cells stimulated with the anti-CD3 antibody for the indicated times were blotted with the anti-B-Raf antibody (*upper panel*). The same membrane was reprobed with the anti-MEK antibody (*lower panel*) to monitor equal protein loading. The data are representative of three reproducible experiments in all analyses. *Ab*, antibody; *IP*, immunoprecipitation.

B-Raf Activation and Subsequently Sustained ERK Activation Is Required for Full IL-2 Production—Since IL-2 production is one of the most critical events of ERK-mediated T cell activation, we first utilized the reporter assay controlled by the IL-2 promoter element to investigate the effect of B-Raf activation on IL-2 promoter activity. Whereas TCR stimulation resulted in induction of luciferase, which reflected the IL-2 promoter activity in wild-type B-Raf-transfected clone (WT30), B-Raf AA significantly attenuated the inducible IL-2 promoter activity (Fig. 5*A*). Indeed, as shown in Fig. 5*B*, TCR stimulation induced a marked increase in IL-2 production in mock-transfected Jurkat cells and in wild-type B-Raf-expressing clones (WT30 and WT34), whereas it was substantially reduced in B-Raf AA-expressing clones (AA2 and AA23).

The data described above clearly indicate that T cells expressing B-Raf AA had defects in sustained ERK activation and subsequent full IL-2 production in comparison with the control cells in response to TCR stimulation. However, whether the sustained ERK activation is directly correlated with the full IL-2 production remained to be solved. To clarify this issue, we investigated the requirement of TCR-mediated sustained ERK activation for the IL-2 production using the pharmacological MEK inhibitor U0126. As shown in Fig. 5*C*, TCR-mediated ERK activation was inhibited by U0126 at the range of 5–10 μM. In addition to ERK activation, IL-2 production provoked by stimulation with immobilized anti-CD3 and CD28 antibodies was markedly blocked by U0126 at the same range of concentrations.

We also examined the effects of B-Raf AA on the magnitude and period of ERK activation stimulated with immobilized anti-CD3 and CD28 antibodies. It must be noted that, as compared with the stimulation by cross-linking of soluble anti-CD3 antibody with the second antibody (Fig. 2*A*), stimulation with immobilized anti-CD3 and -CD28 antibodies resulted in a re-

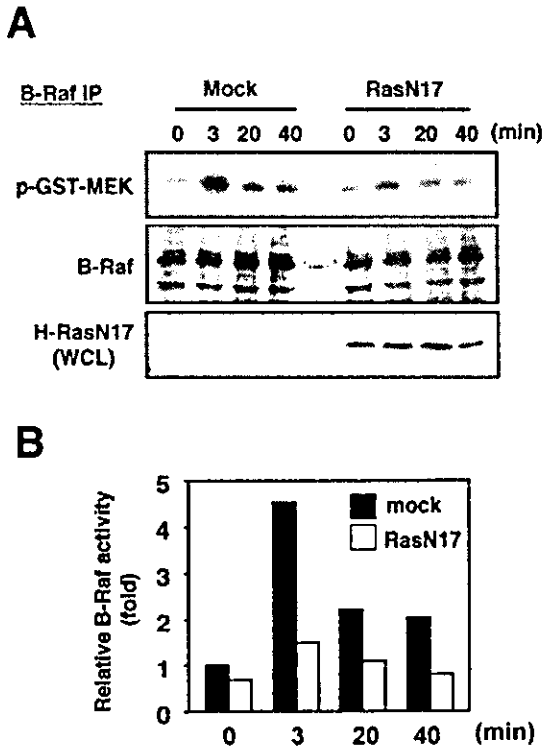

FIG. 3. **Ras-regulated B-Raf activation following TCR stimulation in Jurkat cells.** *A*, TAg-Jurkat cells were transfected with a mock vector or with the RasN17 expression vector, and then these cells were harvested and stimulated with cross-linking of soluble anti-CD3 antibody for the indicated times. Immunoprecipitates from each cell extract with an anti-B-Raf antibody were mixed with the recombinant GST-MEK as a substrate, and *in vitro* kinase reactions for B-Raf were performed. Blotting with an anti-B-Raf antibody showed equal protein loading (*middle panel*). Whole cell lysates (*WCL*) were blotted with anti-H-Ras antibody to monitor the expression of RasN17 (*lower panel*). *B*, the intensity of the GST-MEK phosphorylation by B-Raf immunoprecipitated from mock-transfected (*black bar*) or RasN17-transfected cells (*white bar*) was quantified by densitometric analysis. The relative B-Raf activity at 0 min in mock-transfected cells was assigned to be 1.0. Essentially similar results were obtained in three independent experiments. *IP*, immunoprecipitation.

tardation of ERK activation and extended ERK activation in mock-transfected cells (Fig. 5*D*). Such temporal differences in ERK activation have been reported, and the authors suggested that this phenomenon was due to the difference in TCR occupancy (42). As shown in Fig. 5*D*, in mock-transfected cells, TCR stimulation induced an accumulation of active ERK within 0.5 h, and this lasted for 6 h, whereas the sustained ERK activation over 2 or 3 h was impaired in cells expressing B-Raf AA. The data also confirmed that B-Raf was required for sustained ERK activation. Based on the results of Fig. 5*C*, 5 μM U0126 was used to determine whether the sustained ERK activation that can be suppressed by B-Raf AA, as shown in Fig. 5*D*, was required for the maximal IL-2 production. Continuous treatment of T cells with U0126 over the period of TCR stimulation abolished IL-2 production (Fig. 5*E*). Interestingly, the addition of U0126 after 2 or 4 h of TCR stimulation also reduced IL-2 production to a degree comparable with that of cells treated with U0126 from the beginning of stimulation, although the intense ERK activation was induced for up to 2 h after stimulation. The same condition in which B-Raf AA inhibited the sustained ERK activation can be reproduced by treatment of Jurkat cells with U0126 after 2 or 4 h of TCR stimulation. Therefore, not only the intense ERK activation in the early phase but also the sustained ERK activation in the late phase was necessary for maximal IL-2 production. Concomitantly, these results suggested that the defect of IL-2 production in Jurkat cells expressing B-Raf AA was due to the lack of potential to maintain the TCR-mediated sustained ERK activation although the transient ERK activation was intact.

AP-1 Activation Induced by TCR Ligation Is Not Impaired in Jurkat Cells Expressing B-Raf AA—To define more precisely the biochemical mechanisms underlying the relationship between B-Raf-dependent ERK activation and IL-2 production, we first investigated the TCR-mediated c-Fos induction, one of the downstream targets of ERK (43). As shown in Fig. 6*A*, the expression of c-Fos was induced within 1 h, and its phosphorylation judged by electrophoretic mobility shift was potentiated by TCR stimulation in cells expressing wild-type B-Raf. There was no significant difference in c-Fos induction between Jurkat clones expressing wild-type B-Raf and B-Raf AA up to 3 h (Fig. 6*A*). Next, to examine whether B-Raf contributed to AP-1 activation, we performed a luciferase assay. Consistent with c-Fos induction, the AP-1 promoter activity in response to TCR stimulation in the Jurkat clone expressing B-Raf AA (AA2) was comparable as compared with that of the control clone (WT30) (Fig. 6*B*). Thereby, TCR-mediated c-Fos induction and AP-1 activation seemed to be less dependent on B-Raf.

B-Raf Activity Is Important for TCR-mediated NFAT Activation—The IL-2 production is regulated by nuclear translocation and activation of the NFAT transcription factor cooperating with the AP-1 components c-Fos and c-Jun (7–9). Thus, NFAT-dependent transcriptional events in T cells require the simultaneous activation of multiple Ras effectors such as the ERK and c-Jun N-terminal kinase pathways (44). We analyzed whether TCR-mediated B-Raf activity would influence NFAT activation, using an NFAT-GFP reporter. GFP expression, which is regulated by a promoter corresponding to the NFAT binding site, is increased in a TCR stimulation-dependent manner in mock-transfected cells (Fig. 7*A*, *a*). Comparable transfection efficiency was monitored by co-transfection of a DsRed expression vector (data not shown). In contrast, GFP expression was significantly suppressed in B-Raf AA-expressing cells, suggesting that B-Raf activity is important for the regulation of TCR-mediated NFAT activity. Given that B-Raf regulated TCR-mediated MEK/ERK activation in late phase, there is a possibility that B-Raf activation couples NFAT activation to MEK/ERK activation. For confirmation, we analyzed whether the inhibition of ERK activity in the late phase blocks NFAT reporter activity. As expected, the TCR stimulation-induced GFP expression was reduced by pretreatment with U0126 (Fig. 7*A*, *b*). Furthermore, similar to IL-2 production, the inhibition of NFAT reporter activity was also observed in the presence of U0126 after 2 h of TCR stimulation, although this suppression was less effective than that observed in simultaneous U0126 treatment at the beginning of the TCR stimulation. These results suggested that not only transient but also sustained ERK activation was necessary for the TCR-mediated NFAT activation.

Upon TCR stimulation, NFAT proteins are dephosphorylated by calcineurin, translocate into the nucleus, and then bind to cognate DNA elements (9). Finally, to dissect the mechanism responsible for the B-Raf mediated induction of NFAT activity, we evaluated the nuclear translocation of NFAT protein induced by TCR stimulation. As shown in Fig. 7*B*, the stimulation of mock-transfected Jurkat cells with TCR ligation drove the translocation of NFAT1 and NFAT2 into nucleus at 3 and 5 h of TCR stimulation. In contrast, the substantial nuclear translocation of NFAT1 and NFAT2 could not be observed in B-Raf AA-expressing Jurkat cells under either nonstimulated or TCR-stimulated conditions. Equal loading of nuclear protein in both cells was estimated by blotting of Lamin B as a nuclear

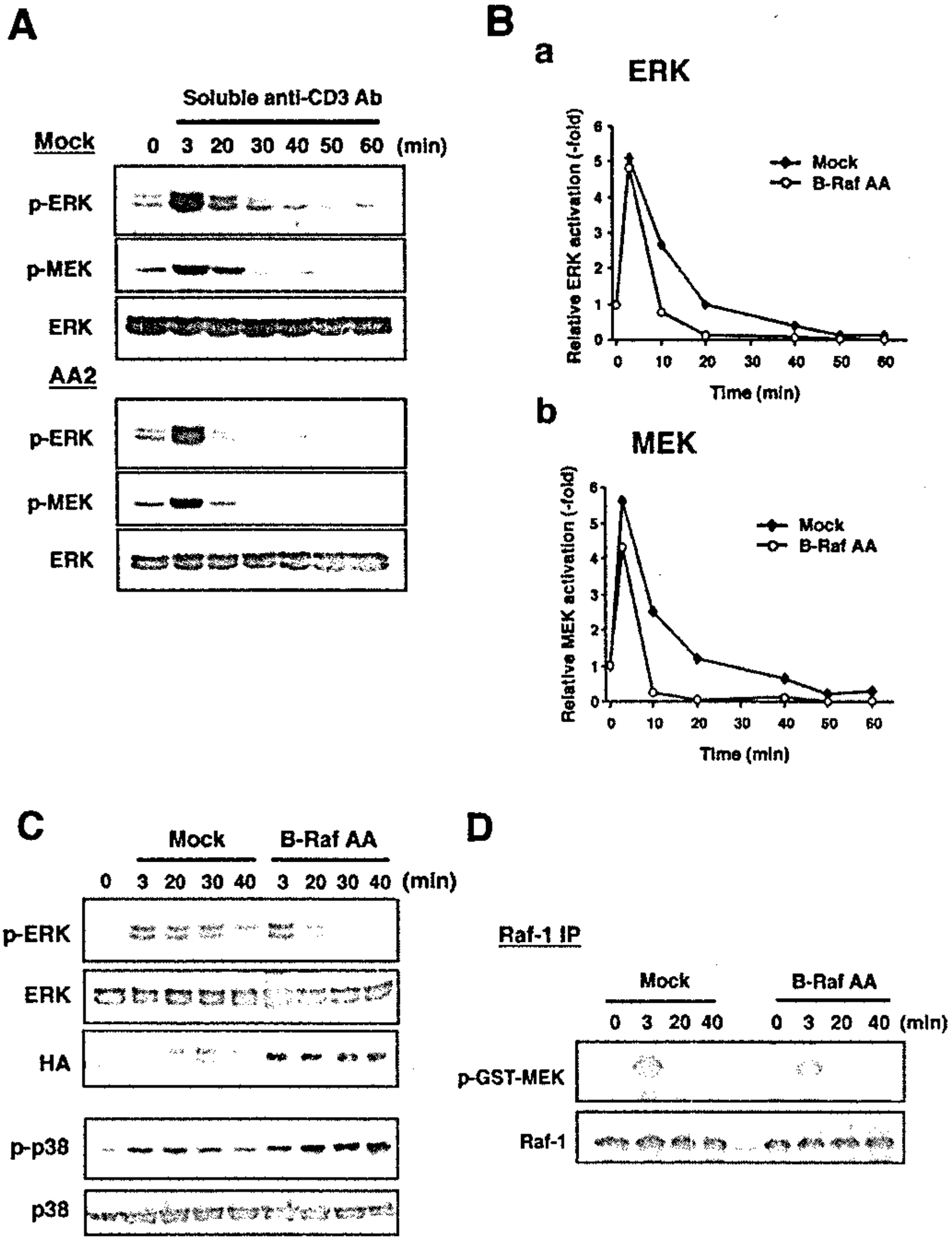

FIG. 4. **Dominant negative B-Raf AA prevented T cells from inducing sustained MEK/ERK activation in response to TCR ligation.** *A*, phosphorylation kinetics of MEK and ERK in Jurkat clones expressing wild-type B-Raf or B-Raf AA (AA2) induced by TCR cross-linking with soluble anti-CD3 antibody. *B*, kinetics of relative amount of phosphorylated ERK (*a*) and MEK (*b*). The relative value of intensity of phosphoprotein bands divided by that of whole ERK bands at each time point observed in mock- or B-Raf AA (AA2)-expressing clone were plotted. The ratio at 0 min was assigned to be 1.0. *C*, Western blotting analyses were done as described in *A* using whole cell lysates from TAg-Jurkat cells transiently transfected with mock or B-Raf AA expression vector and stimulated for the indicated times. Blottings with anti-phospho-ERK, ERK, HA (B-Raf), phospho-p38, or p38 antibodies are shown. *D*, TAg-Jurkat cells transiently transfected with mock vector or with B-Raf AA expression vector were stimulated with TCR cross-linking for the indicated times. *In vitro* kinase assays for Raf-1 were performed using immunoprecipitates from each cell extract with an anti-Raf-1 antibody (*upper panel*). Blotting with anti-Raf-1 antibody indicated equal protein loading (*lower panel*). Each result from three independent experiments was essentially the same, and one is shown.

marker. It is most likely that the defect of NFAT activity in B-Raf AA expressing cells was due to the aberrant nuclear translocation of NFAT1 and NFAT2. Accordingly, these results suggest that TCR-mediated NFAT activation relies on prolonged B-Raf/MEK/ERK activation and that the attenuation of NFAT activation by B-Raf AA reflects the inhibition of TCR-stimulated IL-2 production.

DISCUSSION

Although it is well known that receptor-mediated signals activate the Raf/MEK/ERK cascade, the precise mechanisms of how the TCR signal provokes the cellular response through Raf/MEK/ERK activation remain to be investigated. In mouse models, both Raf-1- and B-Raf-deficient mice resulted in embryonic lethality (20, 45), indicating conclusively that the functions of both Raf isoforms for embryogenesis are not completely overlapping. However, it is poorly understood whether the three Raf isoforms have functional redundancy or if the Raf isoforms play a specific role(s) in T cell activation. Until recently, Raf-1 has been considered to be a major signaling mediator for MEK/ERK activation in TCR-stimulated T cells (27, 46). Our observations provided evidence that the functions of

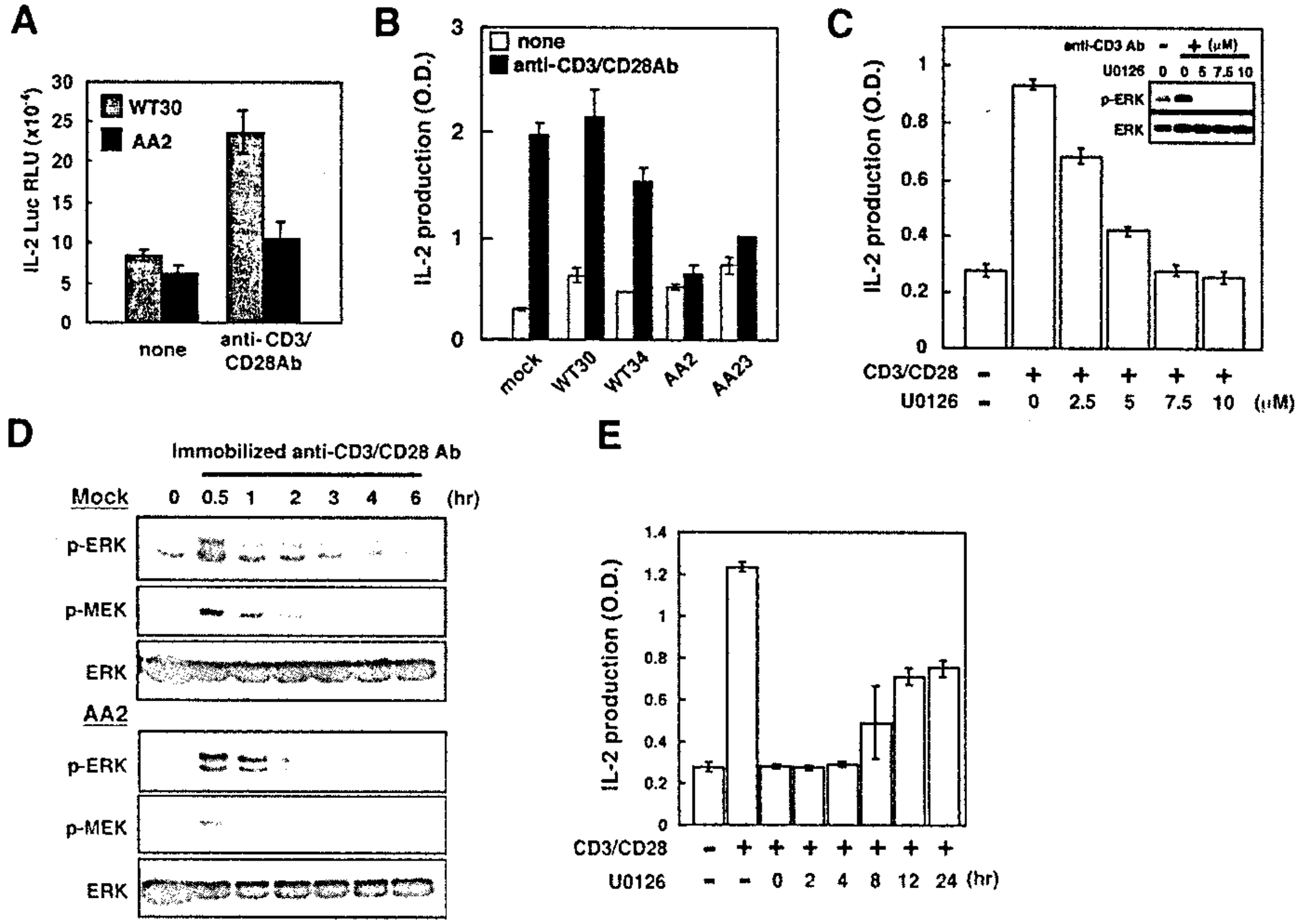

FIG. 5. **Sustained ERK activation controlled by B-Raf is critical in TCR-mediated production of IL-2.** *A*, luciferase assay for IL-2 promoter activity. Jurkat clone expressing wild-type B-Raf (WT30) or B-Raf AA (AA2) was transfected with an IL-2-luciferase construct and incubated with or without immobilized anti-CD3 and anti-CD28 antibodies for 12 h. Each luciferase activity was evaluated and normalized by the co-transfected β-galactosidase activity. *RLU*, relative luciferase unit. *B*, Jurkat clones expressing wild-type B-Raf (WT30 and WT34), B-Raf AA (AA2 and AA23), and mock-transfectant were stimulated with immobilized anti-CD3 and anti-CD28 antibodies for 48 h. IL-2 in the culture supernatants was measured by enzyme-linked immunosorbent assay. *C*, Jurkat cells were pretreated with MEK inhibitor U0126 at the indicated concentrations for 30 min before stimulation and then were stimulated with an anti-CD3 antibody for 3 min, and phosphorylation of ERK was analyzed with Western blotting (*insets*). For measurement of IL-2, Jurkat cells pretreated with U0126 at the indicated concentrations were stimulated with immobilized anti-CD3 and anti-CD28 antibodies for 48 h. IL-2 in the culture supernatants were measured by enzyme-linked immunosorbent assay. *D*, mock-transfected (*upper panel*) or B-Raf AA expressing Jurkat clone (AA2; *lower panel*) were stimulated with the immobilized anti-CD3 and anti-CD28 antibodies for the indicated times. The whole cell extract from each sample was analyzed by blotting with anti-phospho-ERK (*top panel*), phospho-MEK (*middle panel*), or ERK (*bottom panel*) antibodies, respectively. *E*, vehicle (Me_2SO) or U0126 (5 μM) was added to the culture at the indicated times after the beginning of stimulation of Jurkat cells with immobilized anti-CD3 and anti-CD28 antibodies. After 48 h from the start of stimulation, each culture supernatant was harvested, and the IL-2 concentration was measured, as described in *C*. Typical data from three independent and reproducible experiments are presented here.

B-Raf for TCR-mediated activation do not entirely overlap with those of other Raf proteins. We elucidated that B-Raf activation couples Ras with TCR-mediated MEK/ERK activation and is indispensable for prolongation of substantial MEK/ERK activation *in vivo*.

This sustained MEK/ERK activation correlates with duration and strength of B-Raf activity. We considered that activation thresholds and the mechanisms regulating each Raf activity lead to distinct activation kinetics of these two Raf kinases. In agreement with this interpretation, the following observations were reported. Although the activities of both Raf-1 (47) and B-Raf (Fig. 3) were dependent on Ras activity, in addition to Ras, Src family kinases regulated Raf-1 activity (48). Upon activation, Raf-1 was shown to be phosphorylated on some tyrosine, serine, and threonine residues, which fulfill the regulatory functions, and the phosphorylation status of these sites in Raf-1 is different from that of B-Raf. First, the major target site of Src is Tyr^{340} in Raf-1; however, B-Raf activity seemed to be less dependent on Src, and Ras activation is sufficient for B-Raf function because B-Raf lacks the Tyr corresponding to Tyr^{340} in Raf-1 (41, 49). Thus, B-Raf activation requires Ras but not Src to activate MEK/ERK, whereas Raf-1 activation needs the synergy of Ras and Src tyrosine kinase(s) (41, 49). Second, conserved B-Raf Ser^{445}, corresponding to Ser^{338} in Raf-1, which is one of the regulatory phosphorylation sites of Raf activity, is constitutively phosphorylated in fibroblasts (49). These results seem to explain the fact that B-Raf exhibits a higher intrinsic kinase activity in a quiescent situation and, once stimulated, a longer activation period than does Raf-1 in our system and other systems.

It should be noted that the dominant negative mutant of B-Raf (B-Raf AA) did not impair the transient MEK/ERK activation but did suppress the sustained MEK/ERK activation although B-Raf was activated and associated with MEK in both the early and the late phase after TCR stimulation. Why was not MEK/ERK activation in the early phase drastically attenuated by B-Raf AA? The most likely explanation is that Raf-1 can compensate for the defects of B-Raf activation due to the functional redundancy between Raf-1 and B-Raf in early phase. The idea was supported by our observations; the B-Raf AA did not grossly perturb ERK activation when Raf-1 was active in 3–20 min after TCR stimulation (Figs. 2 and 4), suggesting that Raf-1 activity is sufficient to induce ERK activation in the early phase. On the other hand, ERK activation in the late phase (~20 min) was abrogated by B-Raf AA, because the kinase activity of Raf-1 declined, and Raf-1 could no longer compensate for B-Raf activity. Consequently, although we could not exclude the possibility that Raf-1 activity in early phase modulates the TCR-mediated B-Raf activation, our observations led to the model that Raf-1 activity is responsible and sufficient for the early phase MEK/ERK activation, whereas B-Raf activity is essential for the late phase MEK/ERK activation in TCR-stimulated T cells.

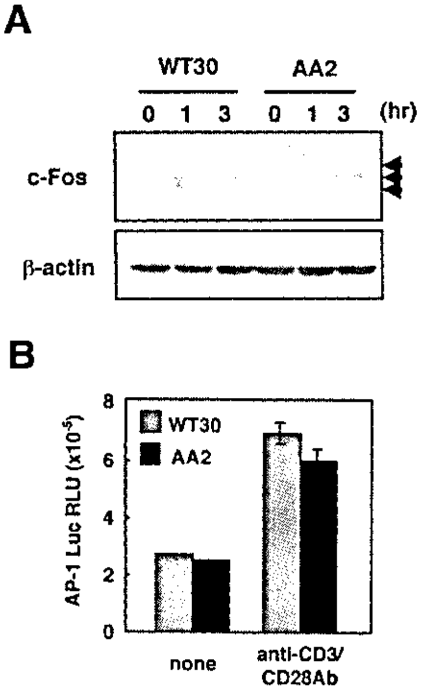

FIG. 6. **B-Raf activity does not influence c-Fos induction and AP-1 activation.** *A*, Western blotting analysis using an anti-c-Fos antibody (*upper panel*). Jurkat clones expressing wild-type B-Raf (WT30) or B-Raf AA (AA2) were stimulated with immobilized anti-CD3 antibody for the indicated times. Blotting with an anti-β-actin antibody indicated equal loading of proteins (*lower panel*). The *arrowheads* indicate the phosphorylated forms of c-Fos. *B*, luciferase assay for AP-1 promoter activity. Jurkat clones expressing wild-type B-Raf (WT30) or B-Raf AA (AA2) together with an AP-1-luciferase construct were stimulated with immobilized anti-CD3 and anti-CD28 antibodies for 8 h followed by a 12-h culture. Each luciferase activity was measured and normalized by the co-transfected β-galactosidase activity. *RLU*, relative luciferase unit. The data are representative of three independent and reproducible experiments. *Ab*, antibody.

ERK activation is critical for the precise outcome of T cell activation, including IL-2 production (7, 15). The marked decrease in IL-2 production in T cells by the expression of B-Raf AA and by the inhibition of the late phase ERK activation using U0126 leads to the conclusion that ERK activation in the late phase regulated by B-Raf was critical for the full IL-2 production in response to TCR stimulation. In view of no defect of TCR-mediated c-Fos induction and AP-1 activation in Jurkat cells expressing B-Raf AA, it was indicated that these events were less dependent on B-Raf activity. In contrast to AP-1 activation, we found that B-Raf AA inhibited TCR-mediated nuclear translocation of NFAT and NFAT-mediated reporter activation (Figs. 6 and 7). The correlation between B-Raf and these transcriptional factors was also noted by Brummer *et al.* (24), who reported that in B-Raf null chicken B cells, B cell receptor-mediated ERK activation was eliminated in only late phase, whereas c-Fos induction was not abrogated. On the contrary, the loss of B-Raf expression resulted in significant defects in the B cell receptor-mediated activation of NFAT transcription factor, suggesting that NFAT activation is regulated by B-Raf in chicken B cells. The selective role of TCR-mediated B-Raf activation in NFAT regulation was consistent with that observed in B cells, and their regulatory mechanisms may be conserved between immunoreceptor-mediated activation in both B and T cells. These results suggest that NFAT-responsible transcriptions and subsequent IL-2 production were dependent on B-Raf and that Raf-1-induced ERK activation in the early phase is not sufficient to provoke these immunoreceptor-mediated activations.

It was expected that the inhibitory effect of B-Raf AA on NFAT activation was due to a defect in sustained ERK activation mediated by B-Raf, because the treatment of Jurkat cells with MEK inhibitor also reduced the NFAT activation. Evi-

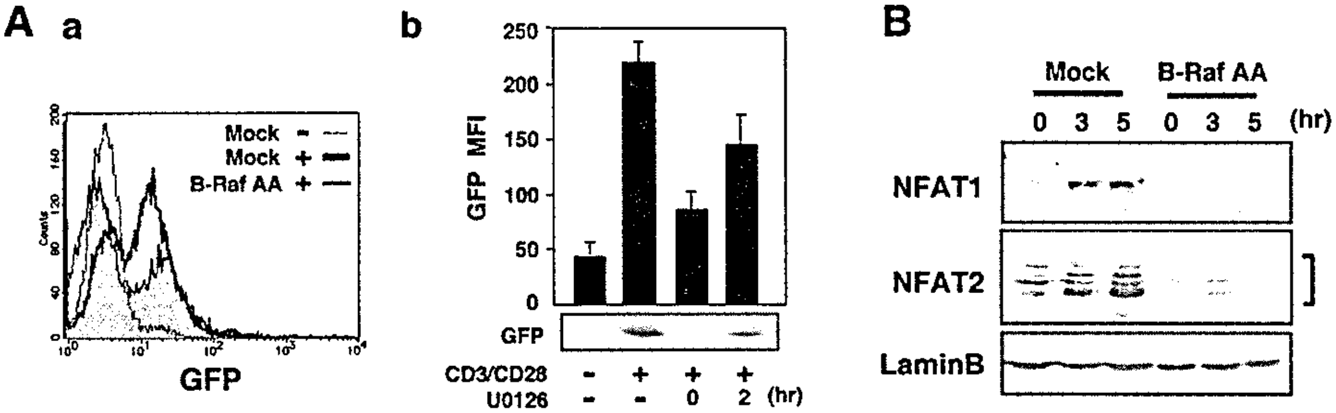

FIG. 7. **B-Raf activity is required for NFAT activation.** *A*, *a*, TAg-Jurkat cells co-transfected with the NFAT-GFP reporter construct and mock or B-Raf AA expression vector were stimulated with (+) or without (−) immobilized anti-CD3 and anti-CD28 antibodies for 9 h. A representative flow cytometric profile for GFP expression is shown. *b*, NFAT-GFP-transfected Jurkat cells were stimulated, and then GFP expression was examined by blotting with anti-GFP antibody (*lower panel*) and flow cytometry (*upper panel*). The *diagram* represents the average of GFP mean fluorescence intensity (*MFI*) obtained from three independent experiments. U0126 (5 μM) was added to the culture at 0 or 2 h after TCR stimulation. *B*, nuclear extracts were isolated from mock- or B-Raf AA-transfected cells stimulated with or without immobilized anti-CD3 and anti-CD28 antibodies for indicated times. Then, the nuclear fractions were separated by SDS-PAGE, and the translocations into nucleus of NFAT1 and NFAT2 were analyzed by Western blotting. Blotting with anti-Lamin B antibody indicated the appropriate nuclear fractionation and protein loading. Essentially similar results were obtained in three independent experiments.

dence has been accumulated that supports the contribution of ERK signaling to NFAT activation. In T cells, the transcriptional activity of NFAT was reported to be regulated by Ras/MEK/ERK acting in synergy with a calcium/calmodulin phosphatase, calcineurin (7, 44). Moreover, the mechanism by which some kinases and phosphatases regulate the NFAT activity implies modulation of nuclear translocation of this factor, its binding to DNA, or transactivation of its target gene expression. Because B-Raf AA abrogated the nuclear localization and transcriptional activity of NFAT, we propose that the model that sustained B-Raf/MEK/ERK activation modulating NFAT-dependent transcription could be achieved by regulation of intrinsic nuclear translocation of NFAT. Supporting this interpretation, it has been reported that ERK1 overexpression augmented the DNA binding activity of NFAT, resulting in NFAT activation in Jurkat cells (50). However, it has been shown that activated ERK binds to and phosphorylates NFAT2, which negatively regulates nuclear translocation and activation of NFAT2 in fibroblasts (51). Conversely, in Jurkat cells, we observed the attenuation of TCR-stimulated nuclear translocation of NFAT by MEK inhibitor.[2] These seemingly discrepant results might be accounted for by use of different systems and cell types. In any case, the formal demonstration of a role for B-Raf and ERK in the regulation of NFAT activation *in vivo* requires more detailed analysis.

It is noteworthy that temporal difference in the Raf-induced ERK activation signal induces qualitatively different cellular responses. In PC12 cells, epidermal growth factor-driven proliferation was coupled with transient ERK activation. On the contrary, neural growth factor-driven differentiation of PC12 cells into sympathetic neurons was induced by sustained ERK activation (10), which was mediated by B-Raf (23). A similar phenomenon was found in T cells. Mariathasan *et al.* (52) demonstrated that in thymocytes, negatively selecting stimuli by agonistic peptides through TCR induced transient and strong ERK activation, resulting in cell death, whereas positively selecting stimuli by the analogue peptides induced sustained and weak ERK activation, resulting in cell survival. In a very recent study, it has been reported that B-Raf but not Raf-1 was activated with TCR stimulation in CD4$^+$CD8$^+$ double positive thymocytes (53). These observations and our findings that B-Raf and Raf-1 activities regulated the strength and the duration of TCR-mediated ERK activation prompted us to consider that the Ras/B-Raf/MEK/ERK pathway also could play important roles in determining the cell fate such as thymocyte differentiation regulated by temporally distinct ERK activity.

In summary, our data suggest that Ras/B-Raf/MEK/ERK can serve as a novel component of signaling pathways that regulate the duration of ERK activity in response to TCR stimulation. B-Raf and ERK activation with a proper duration determines biological outcomes such as IL-2 production in human T cells.

Acknowledgments—We thank Dr. K. L. Guan for generously providing B-Raf constructs, Dr. V. A. Boussiotis for the IL-2 promoter-luciferase reporter construct, Dr. R. M. Niles for the AP-1-luciferase reporter construct, Dr. T. Saito for the NFAT-GFP reporter construct, Dr. Y. Takai for the GST-MEK expression construct, and Dr. G. R. Crabtree for the TAg-Jurkat cells. We also thank M. Ohara for helpful comments.

REFERENCES

1. Kane, L. P., Lin, J., and Weiss, A. (2000) *Curr. Opin. Immunol.* **12,** 242–249
2. Genot, E., and Cantrell, D. A. (2000) *Curr. Opin. Immunol.* **12,** 289–294
3. D'Ambrosio, D., Cantrell, D. A., Frati, L., Santoni, A., and Testi, R. (1994) *Eur. J. Immunol.* **24,** 616–620
4. Carey, K. D., Dillon, T. J., Schmitt, J. M., Baird, A. M., Holdorf, A. D., Straus, D. B., Shaw, A. S., and Stork, P. J. (2000) *Mol. Cell. Biol.* **20,** 8409–8419
5. Katagiri, K., Hattori, M., Minato, N., and Kinashi, T. (2002) *Mol. Cell. Biol.* **22,** 1001–1015
6. Rincon, M. (2001) *Curr. Opin. Immunol.* **13,** 339–345
7. Whitehurst, C. E., and Geppert, T. D. (1996) *J. Immunol.* **156,** 1020–1029
8. Faris, M., Kokot, N., Lee, L., and Nel, A. E. (1996) *J. Biol. Chem.* **271,** 27366–27373
9. Hogan, P. G., Chen, L., Nardone, J., and Rao, A. (2003) *Genes Dev.* **17,** 2205–2232
10. Marshall, C. J. (1995) *Cell* **80,** 179–185
11. Bommhardt, U., Scheuring, Y., Bickel, C., Zamoyska, R., and Hunig, T. (2000) *J. Immunol.* **164,** 2326–2337
12. van den Brink, M. R., Kapeller, R., Pratt, J. C., Chang, J. H., and Burakoff, S. J. (1999) *J. Biol. Chem.* **274,** 11178–11185
13. Pages, G., Guerin, S., Grall, D., Bonino, F., Smith, A., Anjuere, F., Auberger, P., and Pouyssegur, J. (1999) *Science* **286,** 1374–1377
14. Mariathasan, S., Ho, S. S., Zakarian, A., and Ohashi, P. S. (2000) *Eur. J. Immunol.* **30,** 1060–1068
15. Li, Y. Q., Hii, C. S., Der, C. J., and Ferrante, A. (1999) *Immunology* **96,** 524–528
16. Hagemann, C., and Rapp, U. R. (1999) *Exp. Cell Res.* **253,** 34–46
17. Magnuson, N. S., Beck, T., Vahidi, H., Hahn, H., Smola, U., and Rapp, U. R. (1994) *Semin. Cancer Biol.* **5,** 247–253
18. Eychene, A., Dusanter-Fourt, I., Barnier, J. V., Papin, C., Charon, M., Gisselbrecht, S., and Calothy, G. (1995) *Oncogene* **10,** 1159–1165
19. Barnier, J. V., Papin, C., Eychene, A., Lecoq, O., and Calothy, G. (1995) *J. Biol. Chem.* **270,** 23381–23389
20. Wojnowski, L., Zimmer, A. M., Beck, T. W., Hahn, H., Bernal, R., Rapp, U. R., and Zimmer, A. (1997) *Nat. Genet.* **16,** 293–297
21. Papin, C., Denouel-Galy, A., Laugier, D., Calothy, G., and Eychene, A. (1998) *J. Biol. Chem.* **273,** 24939–24947
22. Vaillancourt, R. R., Gardner, A. M., and Johnson, G. L. (1994) *Mol. Cell. Biol.* **14,** 6522–6530
23. York, R. D., Yao, H., Dillon, T., Ellig, C. L., Eckert, S. P., McCleskey, E. W., and Stork, P. J. (1998) *Nature* **392,** 622–626
24. Brummer, T., Shaw, P. E., Reth, M., and Misawa, Y. (2002) *EMBO J.* **21,** 5611–5622
25. Erhardt, P., Schremser, E. J., and Cooper, G. M. (1999) *Mol. Cell. Biol.* **19,** 5308–5315
26. Peraldi, P., Frodin, M., Barnier, J. V., Calleja, V., Scimeca, J. C., Filloux, C., Calothy, G., and Van Obberghen, E. (1995) *FEBS Lett.* **357,** 290–296
27. Owaki, H., Varma, R., Gillis, B., Bruder, J. T., Rapp, U. R., Davis, L. S., and Geppert, T. D. (1993) *EMBO J.* **12,** 4367–4373
28. Northrop, J. P., Ullman, K. S., and Crabtree, G. R. (1993) *J. Biol. Chem.* **268,** 2917–2923
29. Chen, Y. Z., Matsushita, S., and Nishimura, Y. (1996) *J. Immunol.* **157,** 3783–3790
30. Irie, A., Chen, Y. Z., Tsukamoto, H., Jotsuka, T., Masuda, M., and Nishimura, Y. (2003) *Eur. J. Immunol.* **33,** 1497–1507
31. van den Hoff, M. J., Moorman, A. F., and Lamers, W. H. (1992) *Nucleic Acids Res.* **20,** 2902
32. Ohtsuka, T., Shimizu, K., Yamamori, B., Kuroda, S., and Takai, Y. (1996) *J. Biol. Chem.* **271,** 1258–1261
33. Zhang, B. H., and Guan, K. L. (2000) *EMBO J.* **19,** 5429–5439
34. Boussiotis, V. A., Freeman, G. J., Berezovskaya, A., Barber, D. L., and Nadler, L. M. (1997) *Science* **278,** 124–128
35. Huang, Y., Boskovic, G., and Niles, R. M. (2003) *J. Cell. Physiol.* **194,** 162–170
36. Ohtsuka, M., Arase, H., Takeuchi, A., Yamasaki, S., Shiina, R., Suenaga, T., Sakurai, D., Yokosuka, T., Arase, N., Iwashima, M., Kitamura, T., Moriya, H., and Saito, T. (2004) *Proc. Natl. Acad. Sci. U. S. A.* **101,** 8126–8131
37. Uemura, Y., Senju, S., Maenaka, K., Iwai, L. K., Fujii, S., Tabata, H., Tsukamoto, H., Hirata, S., Chen, Y. Z., and Nishimura, Y. (2003) *J. Immunol.* **170,** 947–960
38. Vossler, M. R., Yao, H., York, R. D., Pan, M. G., Rim, C. S., and Stork, P. J. (1997) *Cell* **89,** 73–82
39. Xiang, X., Zang, M., Waelde, C. A., Wen, R., and Luo, Z. (2002) *J. Biol. Chem.* **277,** 44996–45003
40. Chong, H., Lee, J., and Guan, K. L. (2001) *EMBO J.* **20,** 3716–3727
41. Marais, R., Light, Y., Paterson, H. F., Mason, C. S., and Marshall, C. J. (1997) *J. Biol. Chem.* **272,** 4378–4383
42. Borovsky, Z., Mishan-Eisenberg, G., Yaniv, E., and Rachmilewitz, J. (2002) *J. Biol. Chem.* **277,** 21529–21536
43. Deng, T., and Karin, M. (1994) *Nature* **371,** 171–175
44. Genot, E., Cleverley, S., Henning, S., and Cantrell, D. (1996) *EMBO J.* **15,** 3923–3933
45. Wojnowski, L., Stancato, L. F., Zimmer, A. M., Hahn, H., Beck, T. W., Larner, A. C., Rapp, U. R., and Zimmer, A. (1998) *Mech. Dev.* **76,** 141–149
46. Taylor-Fishwick, D. A., and Siegel, J. N. (1995) *Eur. J. Immunol.* **25,** 3215–3221
47. Wotton, D., Ways, D. K., Parker, P. J., and Owen, M. J. (1993) *J. Biol. Chem.* **268,** 17975–17982
48. Pathan, N. I., Ashendel, C. L., Geahlen, R. L., and Harrison, M. L. (1996) *J. Biol. Chem.* **271,** 30315–30317
49. Mason, C. S., Springer, C. J., Cooper, R. G., Superti-Furga, G., Marshall, C. J., and Marais, R. (1999) *EMBO J.* **18,** 2137–2148
50. Park, J. H., and Levitt, L. (1993) *Blood* **82,** 2470–2477
51. Porter, C. M., Havens, M. A., and Clipstone, N. A. (2000) *J. Biol. Chem.* **275,** 3543–3551
52. Mariathasan, S., Zakarian, A., Bouchard, D., Michie, A. M., Zuniga-Pflucker, J. C., and Ohashi, P. S. (2001) *J. Immunol.* **167,** 4966–4973
53. Reynolds, L. F., de Bettignies, C., Norton, T., Beeser, A., Chernoff, J., and Tybulewicz, V. L. (2004) *J. Biol. Chem.* **279,** 18239–18246

---

[2] H. Tsukamoto, A. Irie, and Y. Nishimura, unpublished data.

Mouse Homologue of a Novel Human Oncofetal Antigen, Glypican-3, Evokes T-Cell–Mediated Tumor Rejection without Autoimmune Reactions in Mice

Tetsuya Nakatsura,[1] Hiroyuki Komori,[1,2]
Tatsuko Kubo,[3] Yoshihiro Yoshitake,[1]
Satoru Senju,[1] Toyomasa Katagiri,[4]
Yoichi Furukawa,[4] Michio Ogawa,[2]
Yusuke Nakamura,[4] and Yasuharu Nishimura[1]
Departments of [1]Immunogenetics, [2]Surgery II, and [3]Molecular Pathology, Graduate School of Medical Sciences, Kumamoto University, Kumamoto, and [4]Laboratory of Molecular Medicine, Human Genome Center, Institute of Medical Science, The University of Tokyo, Tokyo, Japan

ABSTRACT

Purpose and Experimental Design:* We recently identified glypican-3 (GPC3) overexpressed specifically in human hepatocellular carcinoma, as based on cDNA microarray analysis of 23,040 genes, and we reported that GPC3 is a novel tumor marker for human hepatocellular carcinoma and melanoma. GPC3, expressed in almost all hepatocellular carcinomas and melanomas, but not in normal tissues except for placenta or fetal liver, is a candidate of ideal tumor antigen for immunotherapy. In this study, we attempted to identify a mouse GPC3 epitope for CTLs in BALB/c mice, and for this, we set up a preclinical study to investigate the usefulness of GPC3 as a target for cancer immunotherapy *in vivo.

***Results:* We identified a mouse GPC3-derived and K^d-restricted CTL epitope peptide in BALB/c mice. Inoculation of this GPC3 peptide-specific CTL into s.c. Colon26 cancer cells transfected with mouse *GPC3* gene (C26/GPC3) led to rejection of the tumor *in vivo*, and i.v. inoculation of these CTLs into sublethally irradiated mice markedly inhibited growth of an established s.c. tumor. Inoculation of bone marrow-derived dendritic cells pulsed with this peptide prevented the growth of s.c. and splenic C26/GPC3 accompanied with massive infiltration of $CD8^+$ T cells into tumors. Evidence of autoimmune reactions was never observed in surviving mice that had rejected tumor cell challenges.**

***Conclusions:* We found the novel oncofetal protein GPC3 to be highly immunogenic in mice and elicited effective antitumor immunity with no evidence of autoimmunity. GPC3 is useful not only for diagnosis of hepatocellular carcinoma and melanoma but also for possible immunotherapy or prevention of these tumors.**

INTRODUCTION

Primary hepatocellular carcinoma is one of the common malignancies throughout the world. Because of the global pandemic of hepatitis B and C infections, the incidence of hepatocellular carcinoma is rapidly on the rise in Asian and Western countries (1). This trend is expected to continue for the next 50 years because of the long latency between infection and development of hepatocellular carcinoma. The prognosis of advanced hepatocellular carcinoma remains poor, and effective treatment strategies are urgently needed.

The report of the cloning human melanoma antigen, *MAGE* gene, stated that the human immune system can recognize cancer as a foreign body and can exclude it (2). This genetic approach of T-cell epitope cloning led to identification of a many genes encoding for tumor antigens and antigenic peptides recognized by tumor-reactive CTLs, thereby enhancing the possibility of antigen-specific cancer immunotherapy (3–6). Recently, >1500 types of candidates of tumor antigens have been identified with the SEREX method (7, 8). We also reported cancer antigens identified with this method (9–11). cDNA microarray technology, by which investigators can obtain comprehensive data with respect to gene expression profiles, is rapidly progressing. Studies have shown the usefulness of this technique for identification of novel cancer-associated genes and for classification of human cancers at the molecular level (12–16). We have recently succeeded in identification of a novel cancer rejection antigen specifically expressed in esophageal cancer with cDNA microarray technology (17).

To identify candidates of ideal hepatocellular carcinoma antigen for tumor immunotherapy, which is strongly expressed in almost all hepatocellular carcinomas but not in normal adult tissues, except for immune privilege tissues such as testis and placenta or fetal organs, we used two kinds of data of cDNA microarrays containing 23,040 genes. One is a comparison of expression profiles between 20 hepatocellular carcinomas and their corresponding noncancerous liver tissues (18) and the other is that of various normal human tissues (19). When using these data, we identified *glypican-3* (*GPC3*) overexpressed specifically in hepatocellular carcinoma, and we reported that GPC3 is a novel tumor marker for human hepatocellular carcinoma (20) and melanoma (21). Not only the amino acid sequences but also the expression patterns of human and mouse

---

Received 6/17/04; revised 9/2/04; accepted 9/15/04.
Grant support: Grants-in-Aid 12213111 (Y. Nishmura) and 14770142 (T. Nakatsura) from the Ministry of Education, Science, Technology, Sports and Culture, Japan.
The costs of publication of this article were defrayed in part by the payment of page charges. This article must therefore be hereby marked *advertisement* in accordance with 18 U.S.C. Section 1734 solely to indicate this fact.
Requests for reprints: Yasuharu Nishimura, Department of Immunogenetics, Graduate School of Medical Sciences, Kumamoto University, Kumamoto 860-8556, Japan. Phone: 81-96-373-5310; Fax: 81-96-373-5314; E-mail: mxnishim@gpo.kumamoto-u.ac.jp.
©2004 American Association for Cancer Research.

GPC3 protein were very similar. GPC3 is an oncofetal protein overexpressed in almost all human hepatocellular carcinomas and melanomas (20). Both human and mouse GPC3 are expressed in normal tissues, including placenta and fetal liver, but not in other normal adult tissues. In the present study, we set up preclinical studies to investigate the usefulness of GPC3 as a target for cancer immunotherapy *in vivo*, and we found this oncofetal protein to be highly immunogenic in mice in that it elicited effective antitumor immunity with no evidence of autoimmunity.

MATERIALS AND METHODS

Cell Lines. A subline of BALB/c-derived colorectal adenocarcinoma cell line Colon26, C26 (C20) (22) was provided by Dr. Kyoichi Shimomura (Fujisawa Pharmaceutical Co., Osaka, Japan). B16 and HepG2 were provided by the Cell Resource Center for Biomedical Research Institute of Development, Aging, and Cancer Tohoku University (Sendai, Japan). T2K^d was provided by Dr. Paul M. Allen of Washington University School of Medicine (St. Louis, MO). These cells were maintained *in vitro* in RPMI 1640 or DMEM supplemented with 10% FCS. Expression of H-2K^d was examined with fluorescence-activated cell sorting analysis and an antimouse H-2K^d–specific antibody and a subsequent FITC-labeled antimouse antibody.

Transfection of *GPC3* Gene into Cells. Plasmids, including full-length murine *GPC3* cDNA clones, were purchased (Invitrogen, Osaka, Japan). A cDNA fragment encoding for GPC3 protein was inserted into pCAGGS-IRES-neo-R, a mammalian expression vector containing the chicken β-actin promoter and an internal ribosomal entry site (IRES)-*neomycin N-acetyltransferase* gene cassette. We used the empty pCAGGS-IRES-neo-R plasmid as a control. These cDNAs were transfected into C26 (C20) cells by lipofection, as previously described (10), and selected with G418.

Mice. Female 7-week-old BALB/c mice (H-2^d), purchased from Charles River Japan (Yokohama, Japan), were kept in the Center for Animal Resources and Development of Kumamoto University and handled in accordance with the animal care policy of Kumamoto University.

Identification of a CTL Epitope in BALB/c Mice. Peptides were purchased from biologica (Tokyo, Japan), and their purity, as estimated by high-performance liquid chromatography, was >95%. The immunizations were done as follows: we primed the mice with 50 μg of each 12 kinds of GPC3-derived peptides emulsified in 50 μL of complete Freund's adjuvant (Sigma, Tokyo, Japan) diluted with 50 μL of saline s.c. into the left flank and boosted these mice with the same peptides emulsified in incomplete Freund's adjuvant by the same method used for priming 7 days after priming. Splenocytes removed from mice 7 days after the last immunization were harvested, depleted of RBCs by hypotonic lysis, and cultured in 24-well culture plates (2.5×10^6/well) in 45% RPMI/45% AIMV/10% FCS supplemented with recombinant human interleukin 2 (100 units/mL), 2-mercaptoethanol (50 μmol/L), and each peptide (10 μmol/L). Then, 5 days later, cytotoxicity of these cells directed against target cells was assayed in a standard 6-hour ^{51}Cr release assays (10). We purified CD8$^+$ T cells from bulk CTLs with the MACS system with antimouse CD8α (Ly-2) monoclonal antibody, and these CD8$^+$ CTLs were used for adoptive transfer into BALB/c mice.

Bone Marrow-derived Dendritic Cell (BM-DC) Vaccine. BM-DCs were generated as follows: BM cells (2×10^6) were cultured in RPMI 1640 supplemented with 10% FCS, together with granulocyte macrophage colony-stimulating factor (5 ng/mL) for 7 days in 10-cm plates, and these BM-DCs were pulsed with GPC3-8 peptide (10 μmol/L) at 37°C for 2 hours and used as GPC3-8 peptide-pulsed BM-DC vaccine.

***In vivo* Depletion of CD4$^+$ and CD8$^+$ T Lymphocytes.** The mice were given a total of six i.p. transfers (days −18, −15, −11, −8, −4, and −1) of the ascites (0.1 mL/mouse/transfer) from hybridoma-bearing nude mice. The mAbs used were rat antimouse CD4 (clone GK1.5) and rat antimouse CD8 (clone 2.43). Normal rat IgG (Sigma, St. Louis, MO; 200 μg/mouse/transfer) was used as control. Depletion of T-cell subsets by treatment with monoclonal antibodies was confirmed by flow cytometric analysis of spleen cells, which showed a >90% specific depletion.

Histologic and Immunohistochemical Analysis. Immunohistochemical (23) and immunocytochemical (24) detections of GPC3 were done, as described previously. We purchased Human, Normal Organs, and Cancers, Tissue Array, BC4 (SuperBioChips Laboratories, Seoul, Korea) and Human Fetal Normal Multi Tissue Slide (BioChain, Hayward, CA) for immunohistochemical analysis. H&E staining and standard methods were used. Immunohistochemical staining of CD8 was done, as described previously (25). For the terminal deoxynucleotidyl transferase-mediated nick end labeling method, we used ApopTag Fluorescein *In Situ* Apoptosis Detection kits (Serologicals Corporation, Norcross, GA).

Statistical Analysis. We analyzed all data with the StatView statistical program for Macintosh (SAS, Inc., Cary, NC) and evaluated the statistical significance with unpaired *t* test. The percentage of overall survival rate was calculated with the Kaplan-Meier method, and statistical significance was evaluated with the Wilcoxon test.

RESULTS

Limited Expression of GPC3 Protein in Both Human and Mouse Fetal Tissues. We and other investigators found GPC3 to be overexpressed in hepatocellular carcinoma (20, 26–31) and melanoma (21), so we did an immunohistochemical analysis of GPC3 with various human and mouse tissues (Fig. 1 and Table 1). The expression patterns of human and mouse GPC3 protein were very similar. GPC3 protein was expressed in placenta and fetal liver, but no or only an expression was observed in all normal adult human and mouse tissues tested, including brain, lung, heart, liver, kidney, mammary gland, spleen, and thymus (Fig. 1, *A* and *B*). The mouse colorectal cancer cell line Colon26 (C26) did not express GPC3, but after stable transfection of mouse *GPC3* genes, GPC3 protein was expressed in C26/GPC3 (Fig. 1*C*). This C26/GPC3 tumor inoculated s.c. into BALB/c mice expressed GPC3 as evidenced in our immunohistochemical analysis (Fig. 1*B*). The expression level of GPC3 protein in C26/GPC3 is not higher than that of human hepatocellular carcinoma (Fig. 1*A*) or the human hepa

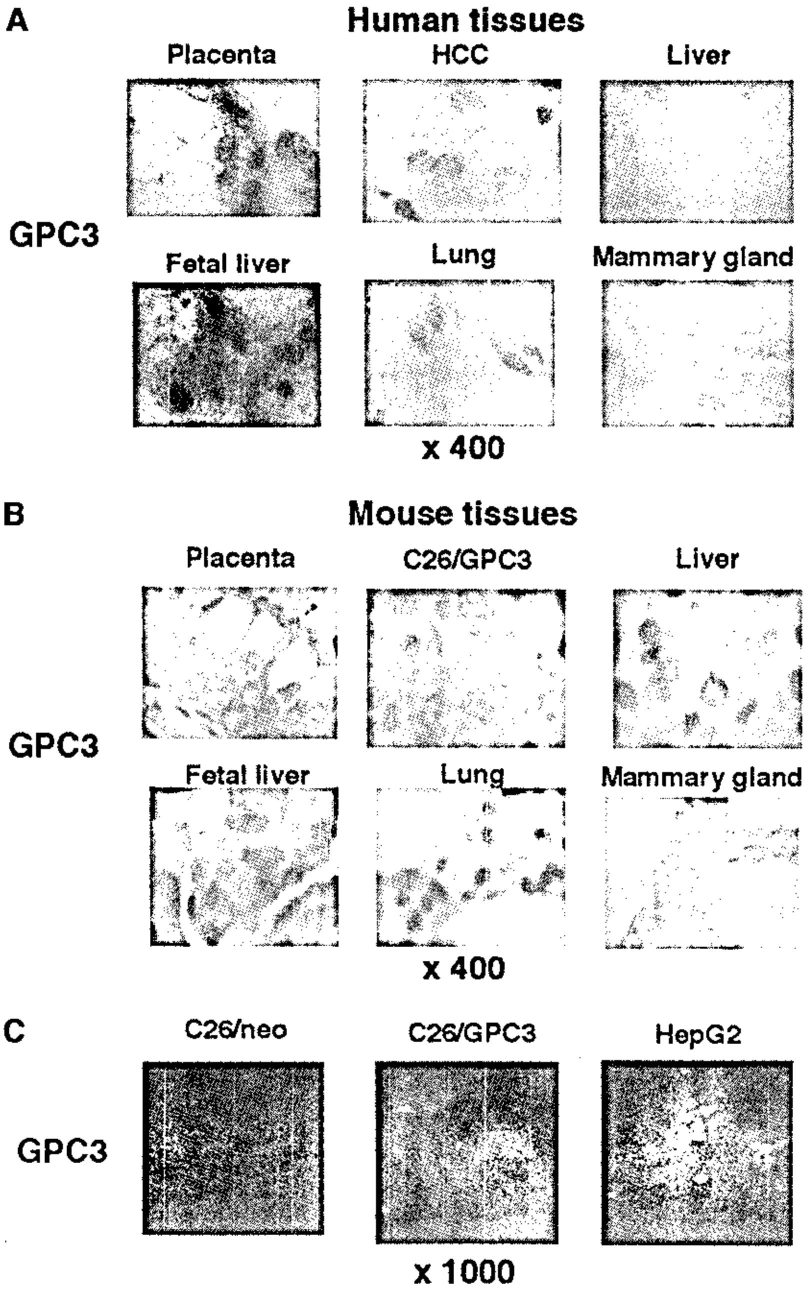

Fig. 1 Expression of GPC3 protein, the candidate of an ideal target for immunotherapy of hepatocellular carcinoma (HCC) and melanoma, in human and mouse tissues and cells. *A* and *B*, expression of GPC3 protein detected by immunohistochemical analysis in various human (*A*) and mouse (*B*) tissues. Objective magnification was 400×. *C*, expression of GPC3 protein detected by FITC-conjugated anti-GPC3 antibodies in HepG2 and GPC3-null mouse colon cancer cell line Colon26 transfected with control vector (C26/neo) or *GPC3* gene (C26/GPC3). Objective magnification was 1000×.

tocellular carcinoma cell line HepG2 (Fig. 1*C*). As a result, the expression levels of GPC3 protein in the human hepatocellular carcinoma, human melanoma, and C26/GPC3 tumor were evidently much higher than those in all adult normal tissues of both human and mouse, including lung and mammary gland, except for placenta and fetal liver (Table 1).

Identification of a GPC3-derived and K^d-restricted CTL Epitope in BALB/c Mice. Structural motifs of peptides bound to human HLA-A24 and mouse K^d are similar. The amino acid sequences of human and mouse GPC3 have a 95% homology. We searched for GPC3-derived peptides of which amino acid sequences were completely shared between human and mouse GPC3. Among these peptides, we selected those carrying binding motifs to both HLA-A24 and K^d molecules, as previously described (10), and prepared 12 different synthetic peptides GPC3-1~12 (Fig. 2*A*). When we tested these peptides for their potential to induce tumor-reactive CTLs *in vitro* from spleen cells derived from mice immunized with GPC3 peptides, only GPC3-8 EYILSLEEL peptide-induced CTLs showed specific cytotoxicity against C26/GPC3 (GPC3+, H-2^d) and T2 cells transfected with the H2-K^d gene (T2K^d) pulsed with GPC3-8 but not against C26 (GPC3−, H-2^d), B16 (GPC3+, H-2^b), and T2K^d cells pulsed with GPC3-7 (Fig. 2, *A* and *B*). These findings indicate

Table 1 The expression levels of GPC3 protein determined by immunohistochemical analysis in various human and mouse tissues

+++*	++	+, +/−	−	−	−
Human hepatocellular carcinoma	Placenta	Lung	Liver	Spleen	Ovary
Human melanoma	Fetal liver	Mammary gland	Brain	Thymus	Uterus
			Heart	Stomach	Prostate
			Kidney	Small intestine	Testis
C26/GPC3 tumor			Pancreas	Colon	C26 tumor

* Expression levels of GPC3 protein determined by immunohistochemical analysis: +++, very strong; ++, strong; +, +/−, weak, −, no or very weak expression.

that this GPC3-8 peptide has the capacity to induce tumor-reactive CTLs and that peptide vaccination primed CTLs reactive to this peptide *in vivo*.

CTL Inoculation Reduced the Growth of C26/GPC3 Tumor in Mice. We determined if these GPC3-8 peptide-induced CTLs were effective against C26/GPC3 tumors inoculated s.c. into BALB/c mice. We separated $CD8^+$ T cells from these GPC3-8 peptide-induced CTLs or from nonspecific cells cultured with interleukin 2, without peptide and injected each of these $CD8^+$ T cells (1×10^7) into each three C26/GPC3 tumors with a diameter of 5 mm (24.2 ± 1.5 mm^2). After 7 days, all three tumors treated with GPC3-8–specific $CD8^+$ CTLs became smaller (15.0 ± 3.2 mm^2), whereas three tumors treated with nonspecific $CD8^+$ T cells became larger (92.3 ± 9.6 mm^2).

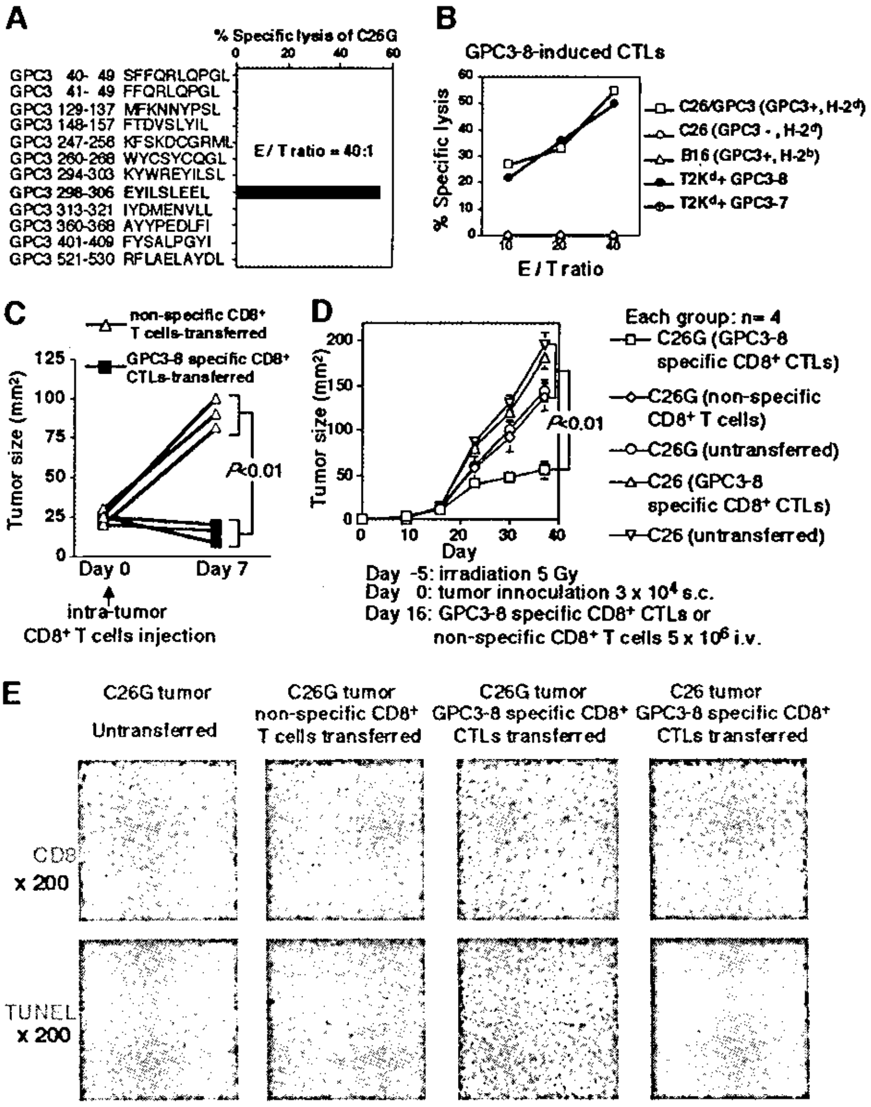

Fig. 2 Identification of a GPC3-derived and K^d-restricted CTL epitope, GPC3-8 EYILSLEEL, and adoptive CTL transfer therapy in BALB/c mice. *A*. BALB/c mice were immunized with 12 GPC3 peptides. Sensitized spleen cells, stimulated *in vitro* with each GPC3 peptide (10 μmol/L) and cultured for 5 days with 100 units/mL interleukin 2, were examined for CTL activity against GPC3-expressing C26/GPC3 cells to identify GPC3-8 EYILSLEEL epitopic peptide. Values represent percent specific lysis calculated based on mean values of triplicate assays. *B*, cytotoxicity of GPC3-8–induced CTLs against various target cells. *C*. $CD8^+$ CTLs (1×10^7) isolated from GPC3-8–induced cells generated as described in *A* or nonspecific cells cultured with interleukin 2, without peptide, were injected into the C26/GPC3 tumor with a diameter of 5 mm in each three mice. The comparison of the tumor size (mm^2) of each three GPC3-8–specific $CD8^+$ CTL-treated tumor and nonspecific $CD8^+$ T-cell–treated tumor was indicated. *D*, suppression of the growth of GPC3-expressing C26/GPC3 tumor inoculated s.c. into sublethally irradiated (5 Gy) mice adoptively transferred with GPC3-8–specific $CD8^+$ CTLs or nonspecific $CD8^+$ T cells. Data are representative of two independent and reproducible experiments. Tumor area was calculated as a product of width and length. Data are presented as mean area of tumor ± SE, and we evaluated the statistical significance with unpaired *t* test. *E*. Immunohistochemical analysis of CD8 or terminal deoxynucleotidyl transferase-mediated nick end labeling-positive cells in specimens of C26/GPC3 or C26 tumor on 21 days after adoptive CTL transfer as done in *D*.

There was a statistical significance ($P < 0.01$) in difference of tumor growth between these two groups (Fig. 2*C*). The results indicate that the GPC3-8 peptide-specific $CD8^+$ CTLs reduced the growth of tumors expressing GPC3.

Sublethal Irradiation of Mice Elicited Effective Antitumor-adoptive Immunity. Antitumor responses could be augmented by T-cell homeostatic proliferation in the periphery, involving expansion of T cells recognizing MHC/tumor antigenic peptide ligands (32–34). To investigate tumor growth in a homeostatic CTL proliferation model, we inoculated C26/GPC3 or C26 cells (3×10^4) s.c. into BALB/c mice 5 days after sublethal irradiation (5 Gy). We injected i.v. 5×10^6 of GPC3-8–induced $CD8^+$ CTLs or nonspecific $CD8^+$ T cells derived from spleen cells cultured with interleukin 2, without peptide for 5 days on day 16 after tumor inoculation, when C26/GPC3 or C26 tumors grew to a diameter of 3 to 4 mm (11.9 ± 0.8 mm^2). Mice were placed into five groups: (*a*) C26/GPC3 (GPC3-8–induced $CD8^+$ CTLs); (*b*) C26/GPC3 (nonspecific $CD8^+$ T cells); (*c*) C26/GPC3 (untransferred); (*d*) C26 (GPC3-8–induced $CD8^+$ CTLs); and (*e*) C26 (untransferred). Measurement of tumor size was continued for 37 days after inoculation of the tumor cells when one untreated mouse died (Fig. 2*D*). Each group included four mice, and we obtained reproducible results in two separate experiments. Mean tumor size on day 37 in C26/GPC3 (CTL) group (51.0 ± 6.0 mm^2) was significantly smaller than that in the other four groups (137.2 ± 16.1, 145.3 ± 12.1, 176.2 ± 10.1, and 195.1 ± 10.2 mm^2; $P < 0.01$). Weight of spleen (0.23 ± 0.03 or 0.25 ± 0.05 g) and spleen cell number ($1.20 \pm 0.40 \times 10^8$ or $1.25 \pm 0.25 \times 10^8$) of GPC3-8–induced $CD8^+$ CTLs or nonspecific $CD8^+$ T-cell–transferred groups, C26/GPC3 (GPC3-8–induced $CD8^+$ CTLs) and C26/GPC3 (nonspecific $CD8^+$ T cells), were larger than those (0.12 ± 0.03 g, $0.23 \pm 0.03 \times 10^8$) of untransferred mice, C26/GPC3 (untransferred) on day 37. These differences were statistically significant ($P < 0.01$), indicating that homeostatic proliferation of T cells had occurred. GPC3-8–induced $CD8^+$ CTLs, but not nonspecific $CD8^+$ T cells, could infiltrate the C26/GPC3 tumor, but not the C26 tumor, and induced apoptosis of C26/GPC3 tumor cells (Fig. 2*E*). Thus, sublethally irradiated lymphopenic mice transfused with syngeneic GPC3-8-reactive CTLs showed tumor growth inhibition for established C26/GPC3 tumors.

Vaccination of GPC3-8 Peptide-pulsed BM-DCs Induced Complete Rejection of C26/GPC3 Tumor Challenge in Mice. The capacity of GPC3-8 peptide-pulsed BM-DCs to prime GPC3-8–specific T cells *in vivo* was analyzed with a s.c. tumor injection model (Fig. 3*B–G*) and an intrasplenic tumor injection model (Fig. 4, *A* and *B*). The protocol of DC vaccination in this study is shown (Fig. 3*A*). In the s.c. tumor injection model, mice were placed into five groups: (*a*) C26/GPC3 (BM-DC+GPC3-8); (*b*) C26/GPC3 (BM-DC); (*c*) C26/GPC3 (untreated); (*d*) C26 (BM-DC+GPC3-8); and (*e*) C26 (untreated). GPC3-8 peptide-pulsed or unpulsed BM-DCs (5×10^5) were injected i.p. into BALB/c mice twice at 7-day intervals. Death never occurred during the vaccination period. Subcutaneous inoculation of C26/GPC3 or C26 cells (3×10^4) into the right flank was given 7 days after the last vaccination. In groups 2 to 5, s.c. tumor appeared 13 days after the inoculation (Fig. 3*B*). Measurement of tumor size was continued until 38 days after inoculation of the tumor cells when one untreated mouse died. All five mice in group 1 completely rejected 3×10^4 of C26/GPC3 cells but not 3×10^4 of C26 cells. Mean tumor size on day 38 in group 1 mice (0 mm^2) was significantly smaller than that in the other four groups 2 to 5 (234.0 ± 28.4, 251.0 ± 60.0, 170.3 ± 26.1, and 229.0 ± 64.2 mm^2, respectively, $P < 0.01$). All mice in groups 2 to 5 died within 88 days after inoculation of the tumor cells (Fig. 3*C*). In group 1, a tumor was not detected in all five mice 150 days after the inoculation. A statistical significance ($P < 0.01$) of difference was found between group 1 and groups 2 to 5. This experiment was repeated with similar results. However, the transfer of GPC3-8 peptide-pulsed BM-DCs showed no efficacy against the established C26G tumor (data not shown). Therefore, the GPC3-8 peptide-pulsed BM-DC therapy has the potential to prevent growth of tumors expressing GPC3 but could not induce regression of an established tumor.

We also inoculated C26/GPC3 or C26 cells s.c. into three surviving mice that completely rejected the first challenges of C26/GPC3 cells by vaccination with BM-DC+GPC3-8 (Fig. 3, *D* and *E*). These mice also rejected rechallenges of C26/GPC3 cells but not C26 until >150 days after the first challenge. In mean tumor size on day 39 and overall survival, the differences between the C26/GPC3-rechallenged group and the other three groups were statistically significant ($P < 0.01$). These results showed that effects of vaccinations with GPC3-8 peptide-pulsed BM-DCs continued for a long time and that the vaccination can prevent recurrence of GPC3-expressing tumors.

Furthermore, we repeated experiment with another control, BM-DC+GPC3-7 (Fig. 3, *F* and *G*). Binding affinity to K^d of GPC3-8 and that of GPC3-7 is predicted to be similar with Bioinformatics & Molecular Analysis Section.[5] As a result, we obtained similar data with experiments with BM-DCs not pulsed with any peptide.

We next analyzed the effect of the vaccination on an intrasplenic tumor injection model (Fig. 4, *A* and *B*). In this model, mice were placed into two groups: (*a*) C26/GPC3 (BM-DC+GPC3-8) and (*b*) C26/GPC3 (untransferred). Each group included five mice, and the results were reproducible in two separate experiments. Seven days after the last vaccination, inoculation of C26/GPC3 cells (1×10^5) into the spleen was done after laparotomy. Eighteen days after the inoculation, we observed the spleens (Fig. 4*A*) and livers (Fig. 4*B*). Tumor nodules appeared in spleens of all five untreated mice, and multiple metastases appeared in two livers (40%) of such mice. On the contrary, all five vaccinated mice completely rejected 1×10^5 of C26/GPC3 cells inoculated into the spleen, and liver metastasis was nil. Differences in weights of spleen and liver and the rates and the numbers of appearance of tumor nodules in spleen were statistically significant among these two groups. Hence, GPC3-8 peptide-pulsed BM-DCs have the capacity to prevent growth in the spleen and possibly liver metastasis of GPC3-expressing tumors.

---

[5] Internet address: http://bimas.dcrt.nih.gov/molbio/hla_bind/.

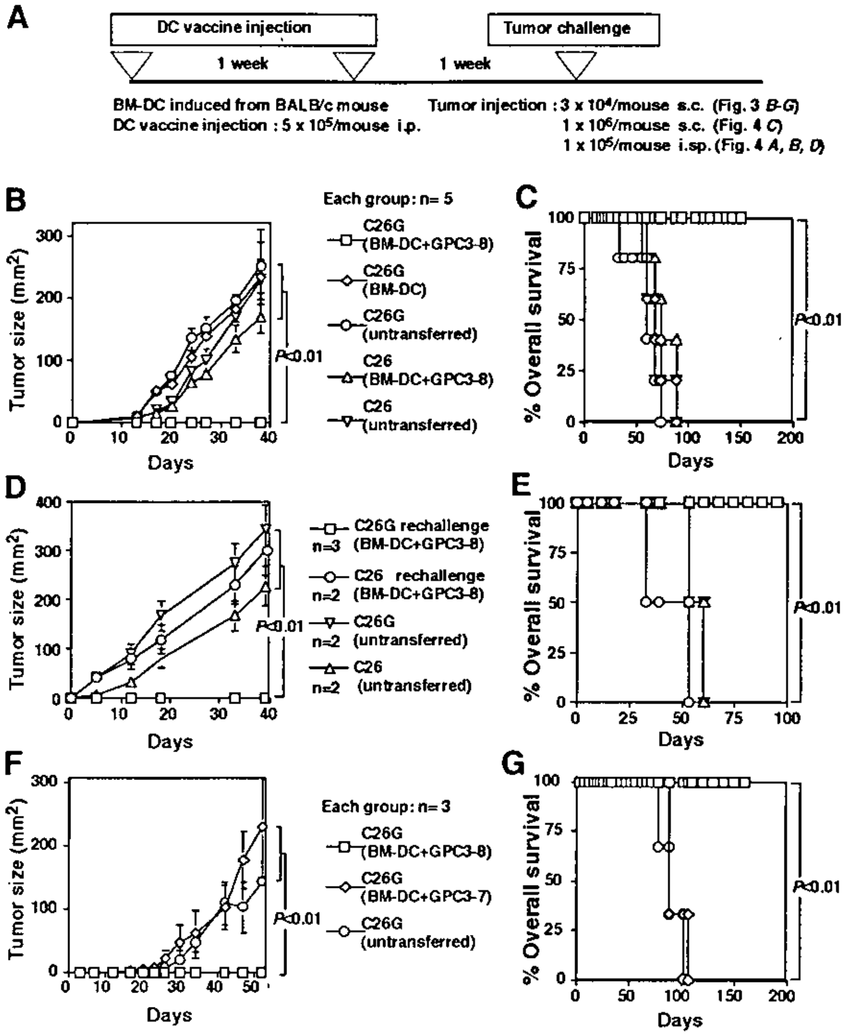

Fig. 3 Mice vaccinated with GPC3-8 peptide-pulsed BM-DCs completely rejected C26/GPC3 tumor challenge. *A*, protocol of peptide-pulsed BM-DC vaccination. *B–G*, s.c. tumor injection model at the first challenge (*B*, *C*, *F*, and *G*) and the rechallenge (*D* and *E*). *B*, *D*, and *F*, suppression of the growth of GPC3-expressing C26/GPC3 tumor inoculated s.c. in mice vaccinated with GPC3-8 peptide-pulsed BM-DCs. Data are representative of two independent and reproducible experiments. Tumor area was calculated as a product of width and length. Data are presented as mean area of tumor ± SE, and we evaluated the statistical significance using unpaired *t* test. *C*, *E*, and *G*, percentage of overall survival was calculated with the Kaplan-Meier method, and the statistical significance of differences between each groups was evaluated with the Wilcoxon test.

Vaccination of GPC3-8 Peptide-pulsed BM-DCs Induced Infiltration of CD8$^+$ T Cells into C26/GPC3 Tumor Cells and Apoptosis of Tumor Cells *In vivo*. In the s.c. tumor injection model, all mice immunized with the BM-DC+GPC3-8 vaccine completely rejected challenges of C26/GPC3 cells (3×10^4). To ascertain that these rejections were induced by CD8$^+$ CTLs, s.c. inoculation of C26/GPC3 or C26 cells (1×10^6) into the right flank was done 7 days after the last vaccination. After tumor formation, we removed the tumor and immunohistochemically stained it with anti-CD8 antibody and the terminal deoxynucleotidyl transferase-mediated nick end labeling method (Fig. 4*C*). Infiltrations of CD8$^+$ T cells into C26/GPC3 tumors and apoptosis of C26/GPC3 tumor cells were observed only in mice vaccinated with GPC3-8 peptide-pulsed BM-DCs but never in mice vaccinated with unpulsed BM-DCs. We also evaluated spleens immunohistochemically with the intrasplenic tumor injection model (Fig. 4*D*). Eighteen days after tumor inoculation, there were fewer CD8$^+$ T cells and terminal deoxynucleotidyl transferase-mediated nick end labeling-positive apoptotic tumor cells in C26/GPC3 tumor nodules in spleens of untreated mice. On the contrary, there were many CD8$^+$ T cells in the considerably enlarged white pulp and some terminal deoxynucleotidyl transferase-mediated nick end labeling-positive apoptotic tumor cells in spleens of mice immunized with the BM-DC+GPC3-8. These results suggest that GPC3-8 peptide-pulsed BM-DCs have the potential to prime a many GPC3-specific CTLs to kill C26/GPC3 tumor cells.

Involvement of CD8$^+$ T Cells in Protection against C26/GPC3 Induced by GPC3-8 Peptide-pulsed BM-DC Vaccination. To determine the role of CD4$^+$ and CD8$^+$ T cells in protection against tumor cells induced by GPC3-8 peptide-pulsed BM-DC vaccination, we depleted mice of CD4$^+$ or CD8$^+$ T lymphocytes by treatment with anti-CD4 or anti-CD8 monoclonal antibody *in vivo*, respectively. With this treatment, >90% of CD4$^+$ and CD8$^+$ T cells were depleted (data not shown). During this procedure, mice were immunized with GPC3-8 peptide-pulsed BM-DCs and challenged with C26/GPC3 cells (each group: $n = 4$). Depletion of CD8$^+$ T cells totally abrogated the protective immunity induced by GPC3-8 peptide-pulsed BM-DCs but that of CD4$^+$ T cells did not do so (data not shown). These results suggest that CD8$^+$ T cells play

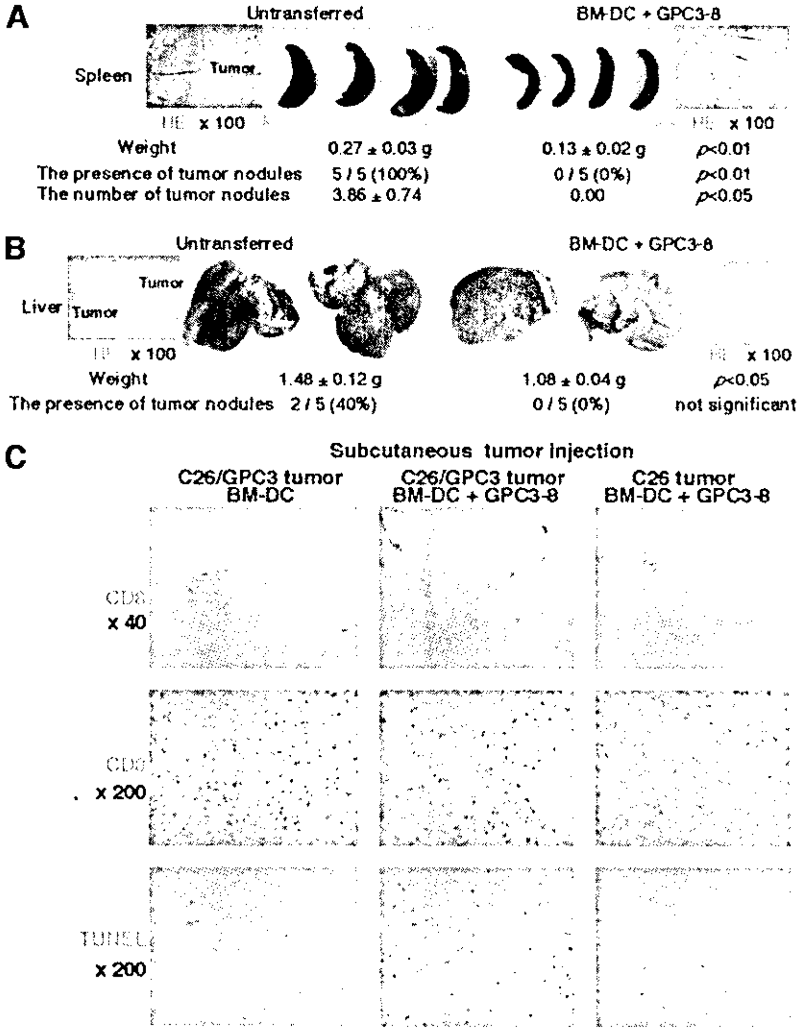
A
Untransferred
BM-DC + GPC3-8
Spleen
Tumor
HE x 100
HE x 100
Weight
0.27 ± 0.03 g
0.13 ± 0.02 g
p<0.01
The presence of tumor nodules
5 / 5 (100%)
0 / 5 (0%)
p<0.01
The number of tumor nodules
3.86 ± 0.74
0.00
p<0.05
B
Untransferred
BM-DC + GPC3-8
Liver
Tumor
Tumor
HE x 100
HE x 100
Weight
1.48 ± 0.12 g
1.08 ± 0.04 g
p<0.05
The presence of tumor nodules
2 / 5 (40%)
0 / 5 (0%)
not significant
C
Subcutaneous tumor injection
C26/GPC3 tumor BM-DC
C26/GPC3 tumor BM-DC + GPC3-8
C26 tumor BM-DC + GPC3-8
CD8 x 40
CD8 x 200
TUNEL x 200

Fig. 4 Vaccination with GPC3-8 peptide-pulsed BM-DCs induced infiltration of CD8$^+$ T cells into C26/GPC3 tumor cells, but not into normal tissues, and induced the apoptosis of C26/GPC3 tumor cells. *A* and *B*, intrasplenic tumor injection model. Eighteen days after inoculation of C26/GPC3 cells (1×10^5) into spleens, the spleens (*A*) and livers (*B*) were observed macroscopically and histologically. *C*, Subcutaneous C26/GPC3 or C26 tumors were analyzed with immunohistochemical staining with anti-CD8 monoclonal antibody and terminal deoxynucleotidyl transferase-mediated nick end labeling (TUNEL) methods 4 days after inoculation of 1×10^6 tumor cells. *D*, Spleens were analyzed with immunohistochemical staining with anti-CD8 monoclonal antibody and TUNEL method 18 days after inoculation of 1×10^5 of C26/GPC3 cells. *E*, The normal tissues of BM-DC+GPC3-8-vaccinated or CTL-treated mice were pathologically and immunohistochemically examined. Objective magnification was 200×. *F*, Placenta and mammary gland of BM-DC+GPC3-8-vaccinated female mice and fetal livers were immunohistochemically analyzed. Objective magnification was 200×.

critical roles in antitumor immunity induced by GPC3-8 peptide-pulsed BM-DCs.

No Evidence of Autoimmune Reactions in Surviving Mice that had Rejected Tumor Cell Challenges. GPC3 expression in normal adult mice was not evident in all tissues tested, which suggests a low risk of damage to normal tissue as a result of immune responses to the GPC3 protein. To evaluate the risk of autoaggression by immunization against GPC3-8, the tissues of BM-DC+GPC3-8 immunized or CTL-treated mice were pathologically examined. Mice shown in Fig. 2, *C* and *D*, were sacrificed at 7 and 21 days after CD8$^+$ T cells transfer, respectively. In addition, mice shown in Figs. 3 and 4*A*–*C* were sacrificed at >150, 25, and 14 days after the last BM-DC+GPC3-8 vaccination, respectively. All mice were apparently healthy without abnormality, suggesting autoimmunity, such as dermatitis, arthritis, or neurologic disorder. The brain, liver, lungs, and heart of these mice were critically scrutinized, and findings were compared with those in normal mice. These tissues had normal structures and cellularity in each of the two mice of groups examined, and pathological changes caused by immune response, such as lymphocyte infiltration or tissue destruction and repair, were nil (Fig. 4*E*). There were no CD8$^+$ T cells in these tissues, which had been immunohistochemically stained (Fig. 4*E*). Although CD8$^+$ T cells infiltrate in the C26/GPC3 tumor 21 days after CD8$^+$ T cells transfer (Fig. 2*E*) and at 14 and 25 days after the last BM-DC vaccination (Fig. 4, *C* and *D*), infiltration of CD8$^+$ T cells was not observed in all adult normal tissues examined at 7 and 21 days after CD8$^+$ T cells transfer (data not shown) and at >150, 25, and 14 days after the last BM-DC vaccination (Fig. 4*E*). These results indicate that lymphocytes stimulated with the GPC3 peptide did not recognize normal self-cells that could express GPC3 at physiologically low levels.

Vaccination of GPC3-8 Peptide-pulsed BM-DCs Induced GPC3-specific CTLs, but did not Induce Damage of Placenta and Fetal Liver Expressing GPC3. In murine tissues, GPC3 protein is expressed in placenta and fetal liver (Fig. 1*B*). To evaluate the risk of autoimmunity against placenta and fetal liver by immunization with BM-DC+GPC3-8, we carried out cross-breeding of BM-DC+GPC3-8–vaccinated female mice with normal male mice and compared events with normal mice pairs. To ascertain induction of GPC3-8-specific CTLs in